Delft University of Technology

Fuzzy Adaptive Prescribed Performance Fault-Tolerant Control for HFVs with Fixed-Time Convergence Guarantee

Dong, Zehong; Li, Yinghui; Lv, Maolong; Zhao, Zilong; Pei, Binbin

Important note
To cite this publication, please use the final published version (if applicable).
Please check the document version above.

Research Article

Fuzzy Adaptive Prescribed Performance Fault-Tolerant Control for HFVs with Fixed-Time Convergence Guarantee

Zehong Dong [iD],[1] Yinghui Li [iD],[2] Maolong Lv,[3] Zilong Zhao,[4] and Binbin Pei[2]

[1]*Graduate School, Air Force Engineering University, Xi'an 710038, China*
[2]*Aviation Engineering School, Air Force Engineering University, Xi'an 710038, China*
[3]*Air Traffic Control and Navigation School, Air Force Engineering University, Xi'an 710051, China*
[4]*Faculty of Electrical Engineering, Mathematics and Computer Science, Delft University of Technology, Van Mourik Broekmanweg 6, 2628 XE Delft, Netherlands*

Correspondence should be addressed to Zehong Dong; dongzehong1995@163.com

A new fixed-time fuzzy adaptive fault-tolerant control methodology is proposed for the longitudinal dynamics of hypersonic flight vehicles (HFVs) in the presence of actuator faults, uncertain dynamics, and external disturbances. In contrast with the conventional fixed-time control schemes that typically contain the fractional powers of errors in their designs, this work develops a low-complexity control structure in the sense of removing the dependence on the need of abovementioned fractional power terms by means of prescribed performance control (PPC) method. Different from the most existing PPC approaches where the initial conditions of tracking errors are required to be known, the newly proposed prescribed performance function (PPF) can relax such restrictions through choosing properly small initial values of PPF. Fuzzy logic systems (FLSs) are employed to handle unknown dynamics, and minimal learning parameter (MLP) technique is incorporated into the design for the purpose of alleviating computation burden. Closed-loop stability is rigorously proved via Lyapunov stability theory, and simulation results are eventually given to validate the effectiveness of the proposed control strategy.

1. Introduction

Hypersonic flight vehicles have already attracted considerable attention due to their advantages of high flight speed, remarkable penetration ability, and cost-effectiveness [1–4]. Nevertheless, the controller design for HFVs remains an intractable issue due to their peculiar features. For example, the engine-airframe structure results in strong couplings between propulsive and aerodynamic forces, and there exist intricate flexible deformation due to the slender geometry of vehicle structure, which influences the aerodynamic characteristics prominently [5]. In addition, the fast time-varying flight environment and the unknown external disturbances lead to frequent parameter variations and model uncertainties, dramatically increasing the difficulty of controller design. To address these problems, many effective methods have been presented, including robust control [5–7], neural/fuzzy control [8–10], prescribed performance control

[11, 12], and disturbance observer-based control [13]. Although these efforts solve the above-mentioned issues to some extent, these results rarely focus on the rate of convergence.

To be specific, only the exponential convergence of tracking error is guaranteed in the aforementioned work, which reveals the convergence time tends to be infinite. From a practical perspective, the rate of convergence is of great significance to the transient tracking performance [14]. Recently, the finite-time tracking control for HFVs is investigated in [14–17], which can make the tracking error converge into the predefined compact set within a finite time. Nevertheless, the convergence time, which is commonly achieved in [14–17], depends on the initial states of the system. It inevitably brings up a problem, that is, the convergence time cannot be accurately settled when the initial states of the system are unknown. To solve such problem, the fixed-time control [18–21] is proposed skillfully,

by which the tracking error can converge into a predefined impact set within a fixed time and the connection between the convergence time and initial states is eliminated.

However, there still exist some shortcomings with the conventional fixed-time tracking control scheme [18–21], where the inequation $\dot{V}(x) \leq -\tau V^p(x) - \varsigma V^q(x) + \kappa$ holds. On the one hand, the derivative of virtual and actual control laws will tend to infinite when the tracking error approaches to zero, giving rise to singularity issues in the control design [21]. On the other hand, when the system encounters the unknown external disturbances [22–26], the dynamic uncertainties [27–32], the system faults [33–36], or input nonlinearities [37], it is complicated to both ensure the fixed-time stability of the system and predetermine the convergence accuracy by selecting the design parameters. As is known to us, the actuator faults not only affect handling performance for HVFs, but even cause closed-loop instability [33–36]. The fault-tolerant control is an inevitable issue for HFVs, due to complex and variable flight environment that may lead to actuator faults, such as control effectiveness decline and drifting. Furthermore, it is well known that the transient and steady-state performances are important to the controller design for HFVs [38]. Nonetheless, the existing PPC for HFVs commonly fails to explicitly contain a convergence time T in the performance function. Thus, it is urgent to develop a new low-complexity fixed-time fault-tolerant control (FTFTC) strategy for HFVs with the prescribed performance.

Motivated by these observations, we present a fixed-time adaptive fuzzy fault-tolerant control scheme for HFVs by utilizing a new prescribed performance function. The contributions mainly contain the follows:

(1) This paper presents a structurally inexpensive FTFTC framework for HFVs in the sense that no fractional powers are involved in the design. There is no fractional power of tracking error in the controller, and thus the singularity problem caused by the derivative of fraction term is removed

(2) By constructing the intermediate control laws and adaptive laws, the adverse impact of actuator faults of HFVs (e.g., loss of effectiveness and drift) is compensated effectively

The remainder of the work is organized as follows. The HFV dynamics and preliminaries are introduced in Section 2. In Section 3, the FLSs-approximator-based FTFTC is designed and the closed-loop stability is verified in Section 4. Section 5 provides simulations to demonstrate the effectiveness of the proposed methods and the work is concluded in Section 6.

A preprint has previously been published by Zehong Dong et al. [39].

2. Problem Formulation and Preliminaries

2.1. Hypersonic Flight Vehicle Dynamics. The longitudinal control-oriented model is originally developed by Parker et al. [40, 41], which can be formulated as

$$\dot{V} = \frac{T \cos(\theta - \gamma) - D}{m} - g \sin \gamma, \dot{h} = V \sin \gamma, \quad (1)$$

$$\dot{\gamma} = \frac{T \sin(\theta - \gamma) + L}{mV} - \frac{g \cos \gamma}{V}, \dot{\theta} = Q, \quad (2)$$

$$\dot{Q} = \frac{M + \tilde{\psi}_1 \ddot{\eta}_1 + \tilde{\psi}_2 \ddot{\eta}_2}{I_{yy}}, \quad (3)$$

$$k_1 \ddot{\eta}_1 = -2\zeta_1 \omega_1 \dot{\eta}_1 - \omega_1^2 \eta_1 + N_1 - \frac{\tilde{\psi}_1 M}{I_{yy}} - \frac{\tilde{\psi}_1 \tilde{\psi}_2 \ddot{\eta}_2}{I_{yy}}, \quad (4)$$

$$k_2 \ddot{\eta}_2 = -2\zeta_2 \omega_2 \dot{\eta}_2 - \omega_2^2 \eta_2 + N_2 - \frac{\tilde{\psi}_2 M}{I_{yy}} - \frac{\tilde{\psi}_1 \tilde{\psi}_2 \ddot{\eta}_1}{I_{yy}}, \quad (5)$$

where T, D, L, M, N_1, and N_2 are expressed as

$$L = \bar{q}SC_L(\alpha, \boldsymbol{\delta}, \boldsymbol{\eta}), D = \bar{q}SC_D(\alpha, \boldsymbol{\delta}, \boldsymbol{\eta}),$$
$$M = z_T T + \bar{q}S\bar{c}C_M(\alpha, \boldsymbol{\delta}, \boldsymbol{\eta}),$$
$$T = \bar{q}S[C_{T,\Phi}(\alpha)v(\Phi) + C_T(\alpha) + \mathbf{C}_T^{\boldsymbol{\eta}}\boldsymbol{\eta}], \quad (6)$$
$$N_i = \bar{q}S[N_i^{\alpha^2}\alpha^2 + N_i^{\alpha}\alpha + N_i^{\delta}\boldsymbol{\delta} + N_i^0 + \mathbf{N}_i^{\boldsymbol{\eta}}\boldsymbol{\eta}], i = 1, 2,$$

where $\alpha = \theta - \gamma$. $\bar{q}$, S, z_T, and $\bar{c}$ denote dynamic press, reference area, thrust moment arm, and reference length. $\boldsymbol{\eta} = [\eta_1, \dot{\eta}_1, \eta_2, \dot{\eta}_2]^T$ denotes the flexible modes. $\boldsymbol{\delta} = [v(\delta_e), \delta_c]^T$, where the deflection of canard δ_c is set to be ganged with $v(\delta_e)$ and $\delta_c = k_{ec}v(\delta_e)$; $k_{ec} = -C_L^{\delta_e}/C_L^{\delta_c}$. This approach was originally proposed in [41] as a way to remove some non-minimum phase characteristics of the dynamics. Considering the actuator fault, the actual output signals of the fuel equivalence ratio and the elevator angular deflection are denoted as $v(\Phi)$ and $v(\delta_e)$, respectively. The aerodynamic model is obtained by curve fitting and can be expressed as

$$C_D(\cdot) = C_D^{\alpha^2}\alpha^2 + C_D^{\alpha}\alpha + C_D^{\delta_e^2}v^2(\delta_e) + C_D^{\delta_e}v(\delta_e) + C_D^{\delta_c}\delta_c$$
$$+ C_D^{\delta_c^2}\delta_c^2 + C_D^0 + \mathbf{C}_D^{\boldsymbol{\eta}}\boldsymbol{\eta}, \quad (7)$$

$$C_M(\cdot) = C_M^{\alpha^2}\alpha^2 + C_M^{\alpha}\alpha + C_M^{\delta_e}v(\delta_e) + C_M^{\delta_c}\delta_c + C_M^0 + \mathbf{C}_M^{\boldsymbol{\eta}}\boldsymbol{\eta}, \quad (8)$$

$$C_L(\cdot) = C_L^{\alpha}\alpha + C_L^{\delta_e}v(\delta_e) + C_L^{\delta_c}\delta_c + C_L^0 + \mathbf{C}_L^{\boldsymbol{\eta}}\boldsymbol{\eta}, \quad (9)$$

$$C_{T,\Phi}(\cdot) = C_{T,\Phi}^{\alpha^3}\alpha^3 + C_{T,\Phi}^{\alpha^2}\alpha^2 + C_{T,\Phi}^{\alpha}\alpha + C_{T,\Phi}^0, \quad (10)$$

$$C_T(\cdot) = C_T^{\alpha^3}\alpha^3 + C_T^{\alpha^2}\alpha^2 + C_T^{\alpha}\alpha + C_T^0, \quad (11)$$

$$\mathbf{C}_j^{\boldsymbol{\eta}} = \left[C_j^{\eta_1}, 0, C_j^{\eta_2}, 0\right], j = T, M, L, D, \quad (12)$$

$$\mathbf{N}_i^{\boldsymbol{\eta}} = \left[N_i^{\eta_1}, 0, N_i^{\eta_2}, 0\right], i = 1, 2, \quad (13)$$

and more detailed definitions can be found in [40–41].

2.2. *The Actuator-Fault Model.* The actuator-fault model is developed by the following formula [34]:

$$\begin{cases} \nu(\Phi) = \omega_\Phi \Phi + \varepsilon_\Phi, \\ \nu(\delta_e) = \omega_{\delta_e} \delta_e + \varepsilon_{\delta_e}, \end{cases} \tag{14}$$

where $\nu(\Phi)$ and $\nu(\delta_e)$ denote the actual output signals of the fuel equivalence ratio and the elevator angular deflection, respectively. $\omega_\bullet$ and $\varepsilon_\bullet$ represent the actual control effectiveness and drift distance, respectively.

Assumption 1. There exists an unknown positive constant $\bar{\varepsilon}_\bullet$ such that $|\varepsilon_\bullet| \leq \bar{\varepsilon}_\bullet$, $0 < \omega_\bullet \leq 1$.

Remark 2. Assumption 1 is commonly applied in FTC research to ensure the controllability of system when the actuator faults occur [34]. During flight, actuator fault inevitably occurs due to multiple factors such as aging and damage of components or screw shedding, which deteriorates the flight performance and even causes the serious flight accident in severe circumstance. Therefore, it is of great significance to consider the possible actuator faults when designing the control strategy. With different values of $\omega_\bullet$ and $\varepsilon_\bullet$, (14) can be divided into the following four cases:

(1) $\omega_\bullet = 1$ and $\varepsilon_\bullet = 0$, representing the fault-free case

(2) $0 < \underline{\omega}_\bullet \leq \omega_\bullet \leq \bar{\omega}_\bullet < 1$ and $\varepsilon_\bullet = 0$, where $\underline{\omega}_\bullet$ and $\bar{\omega}_\bullet$ are unknown positive constants, denoting partial loss of effectiveness

(3) $\omega_\bullet = 1$ and $\varepsilon_\bullet \neq 0$, indicating the bias fault

(4) $0 < \underline{\omega}_\bullet \leq \omega_\bullet \leq \bar{\omega}_\bullet < 1$ and $\varepsilon_\bullet \neq 0$, where $\underline{\omega}_\bullet$ and $\bar{\omega}_\bullet$ are unknown positive constants, signifying that partial loss of effectiveness and bias fault occur at the same time

2.3. *Model Transformation and Decomposition.* According to (1) and (7), V and h are mainly regulated by Φ and δ_e, respectively. To facilitate the controller design, the HFVs dynamics are decomposed into velocity subsystem and altitude subsystem.

Considering the actuator-fault model (14) and inspired by [42, 43], the velocity subsystem is written as

$$\dot{V} = f_V + g_V \nu(\Phi) + d_V, \tag{15}$$

where $f_V = -\bar{q}S/m(C_D^{\alpha^2}\alpha^2 + C_D^\alpha\alpha + C_D^{\delta_e^2}\delta_e^2 + C_D^{\delta_e}\delta_e + C_D^{\delta_c}\delta_c + C_D^{\delta_c^2}\delta_c^2 + C_D^0 + \mathbf{C}_D^\eta \boldsymbol{\eta}) - g\sin\gamma + (\bar{q}S/m)\cos\alpha(C_T^{\alpha^3}\alpha^3 + C_T^{\alpha^2}\alpha^2 + C_T^\alpha\alpha + C_T^0 + \mathbf{C}_T^\eta \boldsymbol{\eta})$, $g_V = (\bar{q}S/m)\cos\alpha(C_{T,\Phi}^{\alpha^3}\alpha^3 + C_{T,\Phi}^{\alpha^2}\alpha^2 + C_{T,\Phi}^\alpha\alpha + C_{T,\Phi}^0)$. f_V and g_V stand for unknown functions due to the time-varying aerodynamic parameters, and d_V represents the external disturbance on velocity.

Considering the actuator-fault model (14) and taking the assumption $\sin(\gamma) \approx \gamma$, $\cos(\gamma) \approx 1$, then the altitude subsystem can be considered as

$$\begin{cases} \dot{h} = V\gamma + d_h, \\ \dot{\gamma} = f_\gamma + g_\gamma\theta + d_\gamma, \\ \dot{\theta} = Q, \\ \dot{Q} = f_Q + g_Q\nu(\delta_e) + d_Q, \end{cases} \tag{16}$$

Similar to velocity subsystem, the functions f_γ, g_γ, f_Q, and g_Q are unknown functions; d_h, d_γ, and d_Q are the external disturbances of altitude subsystem. Along the standard ideas as [10–11], we assume there exist unknown positive functions g_{Vm}, $g_{\gamma m}$, and g_{Qm} such that $0 < g_{Vm} \leq g_V$, $0 < g_{\gamma m} \leq g_\gamma$, and $0 < g_{Qm} \leq g_Q$.

Remark 3. In practice, it is rather difficult to know the values of functions $f_\bullet$, $g_\bullet$, $\in \{V, \gamma, Q\}$ accurately. There are mainly the following reasons: On the one hand, the aerodynamic parameters are constantly changing with the flight environment (i.e., velocity, altitude, and attack of angle), where there inevitably exist measuring errors in the sensors of flight control system [2]. On the other hand, it is impossible to take all flight environment of HFVs into account in a wind tunnel so that we have to rely on curve fitting technology to build the aerodynamic model [7]. Consequently, an exact model for HFVs is difficult to be obtained and in order to facilitate the design of flight control system; we regard $f_\bullet$, $\in \{V, \gamma, Q\}$ as unknown function and regard $g_\bullet$ as unknown positive function.

Assumption 4. See [44]. The reference trajectory $y_{ref}(t)$, together with its i-order derivative $y_{ref}^{(i)}(t)$, is continuous and bounded ($i = 1, 2 \cdots n$).

2.4. *A New Fixed-Time Performance Function*

Definition 5. See [44]. A smooth function $\rho(t)$ is called fixed-time performance function (FTPF), if the following conditions are satisfied:

(1) $\rho(t) > 0$, i.e., $\rho(t)$ is ensured to be a positive function

(2) $\dot{\rho} \leq 0$, that is, $\rho(t)$ is monotonically decreasing

(3) $\lim_{t \to T} \rho(t) = \rho(T)$ and $\rho(t) = \rho(T)$ for any $t > T$, where $\rho(T)$ and T denote an arbitrarily small positive constant and settling time, respectively

According to Definition 5, we construct an FTPF in the form of

$$\rho(t) = \begin{cases} \coth\left(\vartheta\dfrac{t}{T-t} + r\right) - 1 + \rho(T), & 0 \leq t < T \\ \rho(T), & t \geq T. \end{cases} \tag{17}$$

Proof. In view of (17), it can be derived that

$$
\begin{aligned}
\rho(T^-) &= \lim_{t \to T^-}\left[\coth\left(\vartheta\frac{t}{T-t}+r\right)-1+\rho(T)\right] \\
&= \lim_{t \to T^-}\frac{e^{\vartheta(t/(T-t))+r}+e^{-\vartheta(t/(T-t))-r}}{e^{\vartheta(t/(T-t))+r}-e^{-\vartheta(t/(T-t))-r}}-1+\rho(T) \\
&= \rho(T) = \rho(T^+),
\end{aligned}
\tag{18}
$$

that is, $\rho(t)$ is a continuous function. Furthermore, we can deduce that

$$
\begin{aligned}
\dot{\rho}(t) &= -\frac{\vartheta}{T}\left(\frac{T}{T-t}\right)^2\operatorname{csc}h^2\left(\vartheta\frac{t}{T-t}+r\right) \\
&= -\frac{\vartheta}{T}\left(\frac{T}{T-t}\right)^2\left(\frac{2}{e^{\vartheta(t/(T-t))+r}-e^{-\vartheta(t/(T-t))-r}}\right)^2,
\end{aligned}
\tag{19}
$$

when $t < T$, and $\dot{\rho}(t) = 0$ when $t \geq T$. For the sake of simplification, we denote $x = t/T - t$ and the fact $\lim_{t \to T^-} x = +\infty$ holds. Then, we can obtain

$$
\lim_{t \to T^-}\dot{\rho}(t) = \lim_{x \to +\infty}-\frac{4\vartheta}{T}\left(\frac{1+x}{e^{\vartheta x+r}-e^{-\vartheta x-r}}\right)^2.
\tag{20}
$$

With the help of L'Hospital's rule, we get that

$$
\lim_{t \to T^-}\dot{\rho}(t) = \lim_{x \to +\infty}-\frac{4}{T\vartheta}\left(\frac{1}{e^{\vartheta x+r}-e^{-\vartheta x-r}}\right)^2 = \dot{\rho}(T^+).
\tag{21}
$$

Next, $d\rho^2(t)/dt^2$ can be derived as

$$
\begin{aligned}
\frac{d\rho^2(t)}{dt^2} &= -\frac{8\vartheta^2(1+x)^2\left(e^{\vartheta x+r}+e^{-\vartheta x-r}\right)}{T\left(e^{\vartheta x+r}-e^{-\vartheta x-r}\right)^3}-\frac{8\vartheta(1+x)}{T\left(e^{\vartheta x+r}-e^{-\vartheta x-r}\right)^2} \\
&= \frac{T}{4}\dot{\rho}(t)\left(1+\frac{2e^{-\vartheta x-r}}{e^{\vartheta x+r}-e^{-\vartheta x-r}}\right)+\sqrt{|\dot{\rho}(t)|}\frac{4\sqrt{\vartheta/T}}{e^{\vartheta x+r}-e^{-\vartheta x-r}}.
\end{aligned}
\tag{22}
$$

Then, we have $\lim_{t \to T^-}(d\rho^2(t)/dt^2) = (d\rho^2(T^+)/dt^2) = 0$. Similarly, it leads to that $\lim_{t \to T^-}(d\rho^i(t)/dt^i) = (d\rho^i(T^+)/dt^i) = 0, i = 3, \cdots, n$. That is to say, $\rho(t)$ is a smooth function. Furthermore, we can also see that $\dot{\rho}(t) \leq 0$ and the function $\rho(t)$ is continuous at T. Thus, we can conclude that the function $\rho(t)$ is a FTPF. This completes the proof. +. $\square$

Remark 6. We can easily obtain sufficiently large $\rho(0)$ by selecting a sufficiently small r, that is to say, the initial error need not to be known accurately. Consequently, the FTPF without initial error constraint is achieved. Furthermore, we can also conclude that the convergence rate of the error depends on ϑ, which can be seen in Figure 1(a). By setting the steady-state error boundary as $\rho(T) = 1$ and choosing different values of ϑ, we can obtain that a larger ϑ means a faster convergence rate of the error.

Consider the following transformation:

$$
q(t) = \frac{e(t)}{\rho(t)},
\tag{23}
$$

where $e(t)$ represents an error function; the error transformation function is chosen as

$$
z(q) = \frac{q}{1-q^2},
\tag{24}
$$

and we abbreviate $q = q(t)$ there-in-after.

Remark 7. From (24), it can be observed that the inequation $-1 < q < 1$ holds if $z(q)$ is bounded. In view of (23), we conclude that $|e(t)| < |\rho(t)|$ holds as long as $|e(0)| < |\rho(0)|$. Choosing $\vartheta = 0.5$, $r = 0.1$, $T = 6$, and $\rho(T) = 1$, the convergence performance of the proposed FTPF is shown in Figure 1(b). In contrast to traditional PPC [11], where the prescribed performance function is in the form of $\rho(t) = \coth(\vartheta t + r) - 1 + \rho_\infty$, the proposed control scheme explicitly contains a convergence time T in the FTPF. By this means, we can easily preset the convergence time as needed.

2.5. Fuzzy Logic System. In the process of designing the flight controller, the fuzzy logic system is used to estimate the dynamics uncertainties of HFVs. Define a set of fuzzy IF-THEN rules, where the lth IF-THEN rule is written as follows [22, 23, 45, 46]:

$$
\mathscr{R}^l : \text{If } x_1 \text{ is } F_1^l, \text{ and } \cdots \text{ and } x_n \text{ is } F_n^l, \text{ then } y \text{ is } B^l.
\tag{25}
$$

where $\mathbf{x} = [x_1, \cdots, x_n]^T \in \mathbb{R}^n$, and $y \in \mathbb{R}$ are the input and output of the FLSs, respectively, and $F_1^l, \cdots, F_n^l$ and B^l are fuzzy sets in $\mathbb{R}$. Let $F(\mathbf{x})$ be a continuous function defined on a compact set $\Omega_{\mathbf{x}}$. Then, for a given desired level of accuracy $\varepsilon > 0$, there exists a FLS $\mathbf{W}^T\mathbf{S}(\mathbf{x})$ such that $\sup_{\mathbf{x} \in \Omega_{\mathbf{x}}}|F(\mathbf{x}) - \mathbf{W}^T\mathbf{S}(\mathbf{x})| \leq \varepsilon$, where $\mathbf{W} = [w_1, \cdots, w_p]^T$ is the adaptive fuzzy parameter vector in a compact set $\Omega_{\mathbf{W}}$, p is the number of the fuzzy rules, and $\mathbf{S}(\mathbf{x}) = [S_1(\mathbf{x}), \cdots, S_p(\mathbf{x})]^T$ is the fuzzy basis function vector with $S_l(\mathbf{x}) = \prod_{j=1}^m \mu_{F_j^l}(x_j)/\sum_{l=1}^p(\prod_{j=1}^m \mu_{F_j^l}(x_j))$ where $\mu_{F_j^l}(x_j)$ is a fuzzy membership function of the variable x_j in IF-THEN rule. Let $\mathbf{W}^*$ be the optimal parameter vector, which is defined as

$$
\mathbf{W}^* = \arg\min_{\mathbf{W} \in \Omega_{\mathbf{W}}}\left\{\sup_{\mathbf{x} \in \Omega_{\mathbf{x}}}|F(\mathbf{x}) - \mathbf{W}^T\mathbf{S}(\mathbf{x})|\right\}.
\tag{26}
$$

Then, we can further obtain

$$
F(\mathbf{x}) = \mathbf{W}^{*T}\mathbf{S}(\mathbf{x}) + \phi,
\tag{27}
$$

where ϕ is the minimum fuzzy approximation error.

In order to reduce the computational burden, the functions $\ell_V = (\|W_V\|^2/\tilde{g}_{Vm}), \ell_h = (\|W_h\|^2/\tilde{V}_m), \ell_\gamma = (\|W_\gamma\|^2/$
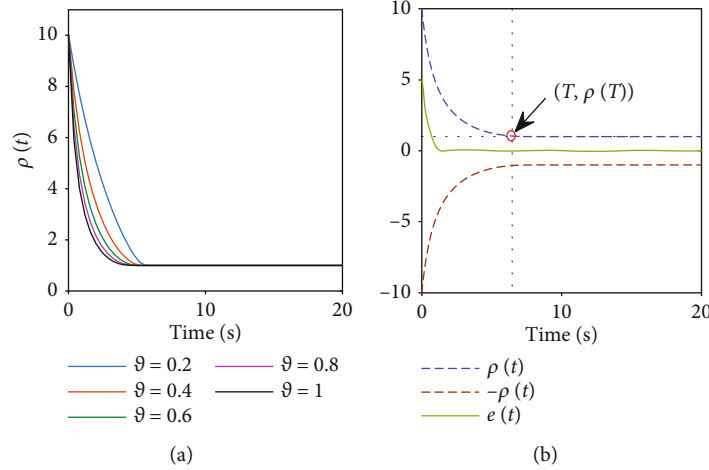
Figure 1: The convergence performance of the proposed FTPF.

g_{ym}), $\ell_\gamma = (\|W_\gamma\|^2/g_{ym})$, $\ell_Q = (\|W_Q\|^2/g_{Qm})$ rather than the ideal weight vectors' elements are estimated in the controller design and stability analysis.

Lemma 8. See [47]. *The hyperbolic tangent function* $\tanh(\bullet)$ *is continuous and differentiable; for* $\forall \varsigma \in R$ *and* $\forall \mu > 0$, *it has*

$$0 \leq |\varsigma| - \varsigma \tanh\left(\frac{\varsigma}{\mu}\right) \leq 0.2785\mu. \tag{28}$$

Lemma 9. See [48]. *For any positive constants* ω *and* δ, *the following inequation holds*

$$0 \leq |\omega| - \frac{\omega^2}{\sqrt{\omega^2 + \delta^2}} \leq \delta. \tag{29}$$

The control objective of this article is to design an fuzzy adaptive tracking controller such that

(1) The velocity and altitude tracking errors are guaranteed to obey the prescribed performance boundaries at all times and finally converge into the predefined residual sets within preassigned time T even in the presentence of actuator faults

(2) All signals of the closed-loop system remain bounded

3. The FTFTC Design

Corresponding to the decomposition in Section 2.3, the control design is also decomposed into a velocity control design and an altitude control design.

3.1. Velocity Controller Design. We first define the velocity tracking error as

$$e_V = V - V_{ref}, \tag{30}$$

where V_{ref} is the velocity reference trajectory. In view of (15), (23), and (24), the time derivative of e_V is

$$\dot{e}_V = f_V + g_V \nu(\Phi) + d_V - \dot{V}_{ref} = \dot{\rho}(t)q + \dot{z}_V \rho(t)\frac{\partial q}{\partial z}. \tag{31}$$

Then, $\dot{z}_V$ can be rewritten as

$$\begin{aligned}
\dot{z}_V &= \frac{f_V + g_V \nu(\Phi) + d_V - \dot{V}_{ref} - \dot{\rho}(t)q}{\rho(t)(\partial q/\partial z)} \\
&= Y_V + E_V(f_V + g_V \nu(\Phi) + d_V - \dot{V}_{ref}),
\end{aligned} \tag{32}$$

with $Y_V = -\dot{\rho}(t)qE_V$, $E_V = (1/\rho(t)(\partial q/\partial z))$.

It can be deduced from (24) that $\partial q/\partial z = (((1-q^2)^2)/(1+q^2)) \leq 1$ when $-1 < q < 1$, and noticing the fact $g_V \geq g_{Vm} > 0$ leads to

$$E_V g_V = \frac{g_V}{\rho(t)(\partial q/\partial z)} \geq \frac{g_{Vm}}{\rho(0)} > 0. \tag{33}$$

Choose the following quadratic function:

$$L_V = \frac{1}{2}z_V^2 + \frac{1}{2\mu_V}\tilde{g}_{Vm}\tilde{\ell}_V^2, \tag{34}$$

where $\tilde{g}_{Vm} = (g_{Vm}/\rho(0))$, $\tilde{\ell}_V = \ell_V - \hat{\ell}_V$, $\hat{\ell}_V$ denotes the estimation of adaptive parameter ℓ_V and μ_V is the positive user-defined parameter.

Utilizing (14) and (31), the time derivative of L_V is

$$\begin{aligned}
\dot{L}_V &= z_V\left(Y_V + E_V f_V + E_V g_V \omega_\Phi \Phi + E_V g_V \varepsilon_\Phi + E_V d_V - E_V \dot{V}_{ref}\right) \\
&\quad - \frac{1}{\mu_V}\tilde{g}_{Vm}\tilde{\ell}_V\hat{\ell}_V.
\end{aligned} \tag{35}$$

Define the nonlinear function

$$F_V = Y_V + E_V f_V + E_V d_V - E_V \dot{V}_{ref} + \frac{1}{2} z_V, \qquad (36)$$

where f_V and d_V are unknown due to the existence of unknown external disturbances and fast time-varying flight environment. An FLSs-approximator is constructed to estimate F_V as

$$F_V = \mathbf{W}_V^{\mathrm{T}} \mathbf{S}_V(\mathbf{x}_V) + \phi_V, \qquad (37)$$

where $\mathbf{x}_V = [V, V_{ref}, \dot{V}_{ref}]^{\mathrm{T}}$. Substituting (36) and (37) into (35), we have

$$\dot{L}_V = z_V \left(\mathbf{W}_V^{\mathrm{T}} \mathbf{S}_V + \phi_V + E_V g_V \omega_\Phi \Phi + E_V g_V \varepsilon_\Phi \right) - \frac{1}{\mu_V} \tilde{g}_{Vm} \tilde{\ell}_V \widehat{\ell}_V - \frac{1}{2} z_V^2. \qquad (38)$$

According to Young's inequation, we can further have

$$z_V \mathbf{W}_V^{\mathrm{T}} \mathbf{S}_V \leq \frac{z_V^2 \|\mathbf{W}_V\|^2 \mathbf{S}_V^{\mathrm{T}} \mathbf{S}_V}{4\tau_V} + \tau_V, \qquad (39)$$
$$z_V \phi_V \leq \frac{1}{2} z_V^2 + \frac{1}{2} \phi_V^2,$$

where τ_V is a positive constant; then, we can rewrite (38) as

$$\dot{L}_V \leq z_V (E_V g_V \omega_\Phi \Phi + E_V g_V \varepsilon_\Phi) + \frac{z_V^2 \|\mathbf{W}_V\|^2 \mathbf{S}_V^{\mathrm{T}} \mathbf{S}_V}{4\tau_V} + \tau_V$$
$$+ \frac{1}{2} \phi_V^2 - \frac{1}{\mu_V} \tilde{g}_{Vm} \tilde{\ell}_V \widehat{\ell}_V. \qquad (40)$$

According to Assumption 1, ω_Φ and ε_Φ are unknown. Therefore, we define the upper and lower bounds of fault parameters to achieve robustness, which are expressed as

$$\underline{\omega}_\Phi = \inf (E_V g_V \omega_\Phi), \vartheta_V = \frac{1}{\underline{\omega}_\Phi}, \qquad (41)$$
$$\xi_V = \sup (E_V g_V \varepsilon_\Phi).$$

Consider the Lyapunov function candidate

$$L_{\bar{V}} = L_V + \frac{1}{2l_V} \underline{\omega}_\Phi \tilde{\vartheta}_V^2 + \frac{1}{2r_V} \tilde{\xi}_V^2, \qquad (42)$$

where $l_V > 0$ and $r_V > 0$ are the parameters to be designed and $\tilde{\vartheta}_V = \vartheta_V - \widehat{\vartheta}_V$ and $\tilde{\xi}_V = \xi_V - \widehat{\xi}_V$ represent estimation errors with $\widehat{\vartheta}_V$ and $\widehat{\xi}_V$ being the estimations of ϑ_V as ξ_V, respectively.

The time derivative of $L_{\bar{V}}$ gives

$$\dot{L}_{\bar{V}} = \dot{L}_V - \frac{1}{l_V} \underline{\omega}_\Phi \tilde{\vartheta}_V \widehat{\vartheta}_V - \frac{1}{r_V} \tilde{\xi}_V \widehat{\xi}_V. \qquad (43)$$

Define $\ell_V = \|\mathbf{W}_V\|^2 / \tilde{g}_{Vm}$ and choose the intermediate control law as

$$\bar{\Phi} = k_V z_V + \frac{z_V \widehat{\ell}_V \mathbf{S}_V^{\mathrm{T}} \mathbf{S}_V}{4\tau_V} + \widehat{\xi}_V \tanh \left(\frac{z_V}{a_V} \right). \qquad (44)$$

It can be induced that

$$\dot{L}_{\bar{V}} \leq z_V E_V g_V \omega_\Phi \Phi + \frac{z_V^2 \ell_V \tilde{g}_{Vm} \mathbf{S}_V^{\mathrm{T}} \mathbf{S}_V}{4\tau_V} + \tau_V + \frac{1}{2} \phi_V^2 - \frac{\omega_\Phi}{l_V} \tilde{\vartheta}_V \widehat{\vartheta}_V$$
$$+ z_V \bar{\Phi} - k_V z_V^2 - \frac{z_V^2 \widehat{\ell}_V \tilde{g}_{Vm} \mathbf{S}_V^{\mathrm{T}} \mathbf{S}_V}{4\tau_V}$$
$$+ \xi_V \left(|z_V| - z_V \tanh \left(\frac{z_V}{a_V} \right) \right) - \frac{\tilde{g}_{Vm}}{\mu_V} \tilde{\ell}_V \widehat{\ell}_V$$
$$+ \frac{1}{r_V} \tilde{\xi}_V \left(r_V z_V \tanh \left(\frac{z_V}{a_V} \right) - \widehat{\xi}_V \right). \qquad (45)$$

Choose the adaptive laws as follows:

$$\widehat{\ell}_V = \frac{\mu_V z_V^2 \mathbf{S}_V^{\mathrm{T}} \mathbf{S}_V}{4\tau_V} - \Gamma_V \widehat{\ell}_V, \qquad (46)$$

$$\widehat{\xi}_V = r_V z_V \tanh \left(\frac{z_V}{a_V} \right) - b_V \widehat{\xi}_V, \qquad (47)$$

$$\widehat{\vartheta}_V = l_V z_V \bar{\Phi} - c_V \widehat{\vartheta}_V, \qquad (48)$$

where $a_V > 0$, $b_V > 0$, and $c_V > 0$ are the parameters to be designed.

Substituting (46)–(48) into (45) yields

$$\dot{L}_{\bar{V}} \leq z_V E_V g_V \omega_\Phi \Phi + \tau_V + \frac{1}{2} \phi_V^2 + \frac{\Gamma_V \tilde{g}_{Vm}}{\mu_V} \tilde{\ell}_V \widehat{\ell}_V$$
$$- \underline{\omega}_\Phi \tilde{\vartheta}_V z_V \bar{\Phi} + \frac{\omega_\Phi c_V}{l_V} \tilde{\vartheta}_V \widehat{\vartheta}_V + z_V \bar{\Phi} - k_V z_V^2 \qquad (49)$$
$$+ \xi_V \left(|z_V| - z_V \tanh \left(\frac{z_V}{a_V} \right) \right) + \frac{b_V}{r_V} \tilde{\xi}_V \widehat{\xi}_V.$$

Now, we design the actual control law as

$$\Phi = -\frac{z_V \widehat{\vartheta}_V^2 \bar{\Phi}^2}{\sqrt{z_V^2 \widehat{\vartheta}_V^2 \bar{\Phi}^2 + \sigma_V^2}}, \qquad (50)$$

where $\sigma_V > 0$ is a predefined constant, which is designed to avoid the singularity issue. According to Young's inequation, one has

$$\tilde{\ell}_V \widehat{\ell}_V = \left(\ell_V - \tilde{\ell}_V \right) \tilde{\ell}_V \leq -\frac{1}{2} \tilde{\ell}_V^2 + \frac{1}{2} \ell_V^2, \qquad (51)$$

$$\tilde{\vartheta}_V \widehat{\vartheta}_V = \left(\vartheta_V - \tilde{\vartheta}_V \right) \tilde{\vartheta}_V \leq -\frac{1}{2} \tilde{\vartheta}_V^2 + \frac{1}{2} \vartheta_V^2, \qquad (52)$$

$$\tilde{\xi}_V \widehat{\xi}_V = \left(\xi_V - \tilde{\xi}_V \right) \tilde{\xi}_V \le -\frac{1}{2} \tilde{\xi}_V^2 + \frac{1}{2} \xi_V^2. \tag{53}$$

Substituting (50)-(53) into (49) and applying Lemma 8 and Lemma 9, we can rewrite (49) as

$$\dot{L}_{\bar{V}} \le -k_V z_V^2 - \frac{1}{2\mu_V} \Gamma_V \tilde{g}_{Vm} \tilde{\ell}_V^2 - \frac{1}{2l_V} \underline{\omega}_\Phi c_V \tilde{\vartheta}_V^2 - \frac{1}{2r_V} b_V \tilde{\xi}_V^2$$
$$+ \frac{1}{2\mu_V} \Gamma_V \tilde{g}_{Vm} \ell_V^2 + \frac{1}{2l_V} \underline{\omega}_\Phi c_V \vartheta_V^2 + \frac{1}{2r_V} b_V \xi_V^2 + \tau_V + \frac{1}{2} \phi_V^2$$
$$+ \underline{\omega}_\Phi \sigma_V + 0.2785 a_V \xi_V. \tag{54}$$

3.2. Altitude Controller Design. In the process of altitude controller design, the backstepping methodology is adopted to deal with complex dynamics. The virtual controllers will be designed at first, and then the intermediate control law the actual control law will be constructed to counteract the impact of actuator fault. To initiate the design process, we first define the following tracking errors:

$$\begin{cases} e_h = h - h_{ref}, & z_\gamma = \gamma - \chi_\gamma, \\ z_\theta = \theta - \chi_\theta, & z_Q = Q - \chi_Q, \end{cases} \tag{55}$$

with χ_γ, χ_θ, and χ_Q representing the virtual control laws.

Step 10. Similarly to velocity controller design, one reaches

$$\dot{e}_h = V\gamma + d_h - \dot{h}_{ref} = \dot{\rho}(t)q + z_h \rho(t) \frac{\partial q}{\partial z}. \tag{56}$$

Then, we have

$$\dot{z}_h = \frac{V\gamma + d_h - \dot{h}_{ref} - \dot{\rho}(t)q}{\rho(t)(\partial q/\partial z)} = Y_h + E_h \left(V\gamma + d_h - \dot{h}_{ref} \right), \tag{57}$$

with

$$Y_h = -\dot{\rho}(t)q E_h, E_h = \frac{1}{\rho(t)(\partial q/\partial z)}. \tag{58}$$

Noting that $(\partial q/\partial z) = (((1 - q^2)^2)/(1 + q^2)) \le 1$ when $-1 < q < 1$ and the fact that $V \ge V_m > 0$ where V_m is minimum permissible flight velocity yields

$$E_h V = \frac{V}{\rho(t)(\partial q/\partial z)} \ge \frac{V_m}{\rho(0)} = \tilde{V}_m > 0. \tag{59}$$

Consider the following Lyapunov function candidate:

$$L_h = \frac{1}{2} z_h^2 + \frac{1}{2\mu_h} \tilde{V}_m \tilde{\ell}_h^2, \tag{60}$$

with $\tilde{\ell}_h = \ell_h - \widehat{\ell}_h$, in which $\widehat{\ell}_h$ denotes the estimation of adaptive parameter ℓ_h and μ_h is the positive design parameter.

The time derivative of L_h gives

$$\dot{L}_h = z_h \left(W_h^T S_h + \phi_h + E_h V\gamma \right) - \frac{1}{\mu_h} \tilde{V}_m \tilde{\ell}_h \widehat{\ell}_h - \frac{1}{2} z_h^2, \tag{61}$$

with $F_h = Y_h + E_h d_h - E_h \dot{h}_{ref} + (1/2)z_h$ being approximated by FLS $W_h^T S_h(\mathbf{x}_h) + \phi_h$, where $\mathbf{x}_h = [h, h_{ref}, \dot{h}_{ref}]^T$.

Applying Young's inequation, it gives

$$z_h W_h^T S_h \le \frac{z_h^2 \| W_h \|^2 S_h^T S_h}{4\tau_h} + \tau_h,$$
$$z_h \phi_h \le \frac{1}{2} z_h^2 + \frac{1}{2} \phi_h^2, \tag{62}$$

where τ_h is a positive constant; noting that $\gamma = z_\gamma + \chi_\gamma$ we can further rewrite (61) as

$$\dot{L}_h \le E_h V z_h z_\gamma + z_h E_h V\chi_\gamma + \frac{z_h^2 \ell_h \tilde{V}_m S_h^T S_h}{4\tau_h} + \tau_h + \frac{1}{2} \phi_h^2 - \frac{1}{\mu_h} \tilde{V}_m \tilde{\ell}_h \widehat{\ell}_h, \tag{63}$$

with the definition of $\ell_h = (\| W_h \|^2 / \tilde{V}_m)$. Choose the virtual control law and updating law as follows:

$$\chi_\gamma = -k_h z_h - \frac{z_h \widehat{\ell}_h S_h^T S_h}{4\tau_h}, \tag{64}$$

$$\widehat{\ell}_h = \frac{\mu_h z_h^2 S_h^T S_h}{4\tau_h} - \Gamma_h \widehat{\ell}_h. \tag{65}$$

Substituting (64)–(65) into (63) yields

$$\dot{L}_h \le -k_h z_h^2 + \frac{1}{\mu_h} \Gamma_h \tilde{V}_m \tilde{\ell}_h \widehat{\ell}_h + E_h V z_h z_\gamma + \frac{1}{2} \phi_h^2 + \tau_h. \tag{66}$$

Step 11. Take the Lyapunov function candidate as

$$L_\gamma = L_h + \frac{1}{2} z_\gamma^2 + \frac{1}{2\mu_\gamma} g_{\gamma m} \tilde{\ell}_\gamma^2. \tag{67}$$

Similar to step 10, by defining $\ell_\gamma = (\| W_h \|^2 / g_{\gamma m})$, the time derivative of L_γ can be formulated as

$$\dot{L}_\gamma = \dot{L}_h + z_\gamma \left(W_\gamma^T S_\gamma + \phi_\gamma + g_\gamma \theta \right) - \frac{1}{\mu_{\gamma m}} g_{\gamma m} \tilde{\ell}_\gamma \widehat{\ell}_\gamma - E_h V z_h z_\gamma - \frac{1}{2} z_\gamma^2, \tag{68}$$

with $F_\gamma = f_\gamma + E_h V z_h + d_\gamma - \dot{\chi}_\gamma + (1/2)z_\gamma$ being approximated by FLS $W_\gamma^T S_\gamma(\mathbf{x}_\gamma) + \phi_\gamma$, where $\dot{\chi}_\gamma = (\partial \chi_\gamma/\partial h)\dot{h} + (\partial \chi_\gamma/\partial \widehat{\ell}_h)\dot{\widehat{\ell}}_h + (\partial \chi_\gamma/\partial h_{ref})\dot{h}_{ref}$ and $\mathbf{x}_\gamma = [h, \gamma, h_{ref}, \dot{h}_{ref}, h_{ref}^{(2)}, \widehat{\ell}_h]^T$.

Design the virtual control law and adaptive law as

$$\chi_\theta = -k_\gamma z_\gamma - \frac{z_\gamma \widehat{\ell}_\gamma \mathbf{S}_\gamma^\mathrm{T} \mathbf{S}_\gamma}{4\tau_\gamma}, \tag{69}$$

$$\dot{\widehat{\ell}}_\gamma = \frac{\mu_\gamma z_\gamma^2 \mathbf{S}_\gamma^\mathrm{T} \mathbf{S}_\gamma}{4\tau_\gamma} - \Gamma_\gamma \widehat{\ell}_\gamma. \tag{70}$$

Based on (66)–(70), we obtain

$$\dot{L}_\gamma \leq -k_h z_h^2 - k_\gamma z_\gamma^2 + \frac{1}{\mu_h}\Gamma_h \tilde{V}_m \tilde{\ell}_h \widehat{\ell}_h + \frac{1}{\mu_\gamma}\Gamma_\gamma g_{\gamma m} \tilde{\ell}_\gamma \widehat{\ell}_\gamma + g_\gamma z_\gamma z_\theta$$
$$+ \frac{1}{2}\phi_h^2 + \frac{1}{2}\phi_\gamma^2 + \tau_h + \tau_\gamma. \tag{71}$$

Step 12. Consider the following Lyapunov function candidate:

$$L_\theta = L_\gamma + \frac{1}{2}z_\theta^2 + \frac{1}{2\mu_\theta}\tilde{\ell}_\theta^2. \tag{72}$$

Defining $\ell_\theta = \|\mathbf{W}_\theta\|^2$, the time derivative of L_θ gives

$$\dot{L}_\theta = \dot{L}_\gamma + z_\theta\big(\mathbf{W}_\theta^\mathrm{T}\mathbf{S}_\theta + \phi_\theta + Q\big) - \frac{1}{\mu_\theta}\tilde{\ell}_\theta \widehat{\ell}_\theta - g_\gamma z_\gamma z_\theta - \frac{1}{2}z_\theta^2, \tag{73}$$

with $F_\theta = g_\gamma z_\gamma - \dot{\chi}_\theta + (1/2)z_\theta$ being approximated by FLS $\mathbf{W}_\theta^\mathrm{T}\mathbf{S}_\theta(\mathbf{x}_\theta) + \phi_\theta$, where $\dot{\chi}_\theta = \sum_{x=h,\gamma}(\partial\chi_\theta/\partial x)\dot{x} + \sum_{x=h,\gamma}(\partial\chi_\theta/\partial\widehat{\ell}_x)\dot{\widehat{\ell}}_x + \sum_{i=0}^{2}(\partial\chi_\theta/\partial h_{ref}^{(i)})h_{ref}^{(i+1)}$ and $\mathbf{x}_\theta = [h, \gamma, \theta, h_{ref}, \dot{h}_{ref}, h_{ref}^{(2)}, h_{ref}^{(3)}, \widehat{\ell}_h, \widehat{\ell}_\gamma]^\mathrm{T}$.

Construct the virtual control law and adaptive law

$$\chi_Q = -k_\theta z_\theta - \frac{z_\theta \widehat{\ell}_\theta \mathbf{S}_\theta^\mathrm{T} \mathbf{S}_\theta}{4\tau_\theta}, \tag{74}$$

$$\dot{\widehat{\ell}}_\theta = \frac{\mu_\theta z_\theta^2 \mathbf{S}_\theta^\mathrm{T} \mathbf{S}_\theta}{4\tau_\theta} - \Gamma_\theta \widehat{\ell}_\theta. \tag{75}$$

From (72)–(75), one has

$$\dot{L}_\theta \leq -k_h z_h^2 - k_\gamma z_\gamma^2 - k_\theta z_\theta^2 + \frac{\Gamma_h \tilde{V}_m}{\mu_h}\tilde{\ell}_h \widehat{\ell}_h + \frac{\Gamma_\gamma g_{\gamma m}}{\mu_\gamma}\tilde{\ell}_\gamma \widehat{\ell}_\gamma + z_\theta z_Q$$
$$+ \frac{\Gamma_\theta}{\mu_\theta}\tilde{\ell}_\theta \widehat{\ell}_\theta + \frac{1}{2}\phi_h^2 + \frac{1}{2}\phi_\gamma^2 + \frac{1}{2}\phi_\theta^2 + \tau_h + \tau_\gamma + \tau_\theta. \tag{76}$$

Step 13. Choose the following Lyapunov function candidate:

$$L_Q = L_\theta + \frac{1}{2}z_Q^2 + \frac{1}{2\mu_Q}g_{Qm}\tilde{\ell}_Q^2. \tag{77}$$

Constructing $\ell_Q = (\|\mathbf{W}_Q\|^2/g_{Qm})$ and taking the derivative of L_Q yield

$$\dot{L}_Q = \dot{L}_\theta + z_Q\big(\mathbf{W}_Q^\mathrm{T}\mathbf{S}_Q + \phi_Q + g_Q\omega_{\delta_e}\delta_e + g_Q\varepsilon_{\delta_e}\big)$$
$$- \frac{1}{\mu_Q}g_{Qm}\tilde{\ell}_Q \widehat{\ell}_Q - z_\theta z_Q - \frac{1}{2}z_Q^2, \tag{78}$$

with $F_Q = f_Q + z_\theta + d_Q - \dot{\chi}_\theta + (1/2)z_Q$ being approximated by FLS $\mathbf{W}_Q^\mathrm{T}\mathbf{S}_Q(\mathbf{x}_Q) + \phi_Q$, where $\dot{\chi}_Q = \sum_{x=h,\gamma,\theta}(\partial\chi_Q/\partial x)\dot{x} + \sum_{x=h,\gamma,\theta}(\partial\chi_Q/\partial\widehat{\ell}_x)\dot{\widehat{\ell}}_x + \sum_{i=0}^{3}(\partial\chi_Q/\partial h_{ref}^{(i)})h_{ref}^{(i+1)}$ and $\mathbf{x}_Q = [h, \gamma, \theta, Q, h_{ref}, \dot{h}_{ref}, h_{ref}^{(2)}, h_{ref}^{(3)}, h_{ref}^{(4)}, \widehat{\ell}_h, \widehat{\ell}_\gamma, \widehat{\ell}_\theta]^\mathrm{T}$.

The upper and lower bounds of fault parameters are defined as

$$\underline{\omega}_{\delta_e} = \inf\big(g_Q\omega_{\delta_e}\big), \vartheta_Q = \frac{1}{\underline{\omega}_{\delta_e}},$$
$$\xi_Q = \sup\big(g_Q\varepsilon_{\delta_e}\big). \tag{79}$$

Construct the Lyapunov function:

$$L_{\bar{Q}} = L_Q + \frac{1}{2l_Q}\underline{\omega}_{\delta_e}\tilde{\vartheta}_Q^2 + \frac{1}{2r_Q}\tilde{\xi}_Q^2, \tag{80}$$

where $l_Q > 0$ and $r_Q > 0$ are designed parameters and $\tilde{\vartheta}_Q = \vartheta_Q - \widehat{\vartheta}_Q$ and $\tilde{\xi}_Q = \xi_Q - \widehat{\xi}_Q$ represent estimation errors with $\widehat{\vartheta}_Q$ and $\widehat{\xi}_Q$ being the estimations of ϑ_Q and ξ_Q, respectively. Choose the intermediate control law and adaptive laws as follows:

$$\bar{\delta}_e = k_Q z_Q + \frac{z_Q \widehat{\ell}_Q \mathbf{S}_Q^\mathrm{T} \mathbf{S}_Q}{4\tau_Q} + \widehat{\xi}_Q \tanh\left(\frac{z_Q}{a_Q}\right), \tag{81}$$

$$\dot{\widehat{\ell}}_Q = \frac{\mu_Q z_Q^2 \mathbf{S}_Q^\mathrm{T} \mathbf{S}_Q}{4\tau_Q} - \Gamma_Q \widehat{\ell}_Q, \tag{82}$$

$$\dot{\widehat{\xi}}_Q = r_Q z_Q \tanh\left(\frac{z_Q}{a_Q}\right) - b_Q \widehat{\xi}_Q, \tag{83}$$

$$\dot{\widehat{\vartheta}}_Q = l_Q z_Q \bar{\delta}_e - c_Q \widehat{\vartheta}_Q, \tag{84}$$

where k_Q, τ_Q, a_Q, b_Q, and c_Q are designed positive parameters.

Finally, we choose the actual control law as

$$\delta_e = -\frac{z_Q \widehat{\vartheta}_Q^2 \bar{\delta}_e^2}{\sqrt{z_Q^2 \widehat{\vartheta}_Q^2 \bar{\delta}_e^2 + \sigma_Q^2}}, \tag{85}$$

where $\sigma_Q > 0$ is a predefined constant. Following similar analysis to velocity subsystem, we can further deduce that
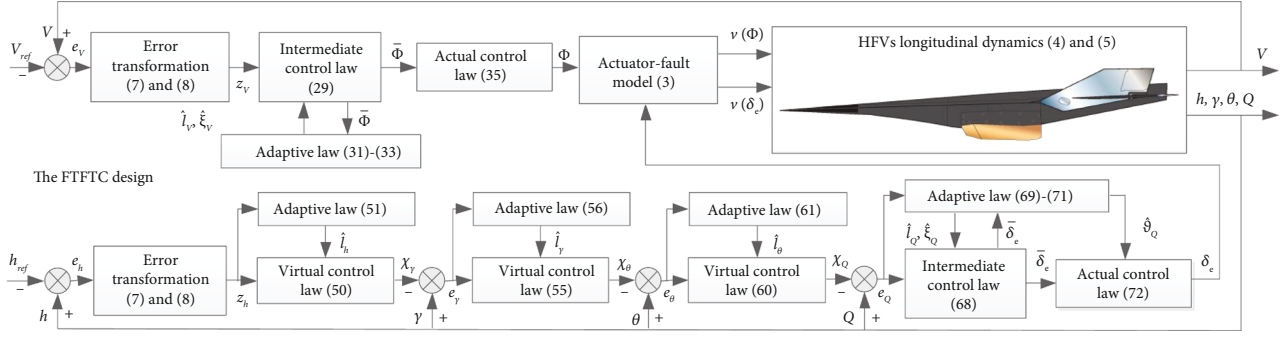
Figure 2: Overall fixed-time tolerant-control scheme for HFVs.

Table 1: The initial states.

States	Value	Units
V	7700	ft/s
h	85000	ft
γ	0	deg
θ	1.6325	deg
Q	0	deg/s
η_1	0.97	ft slugs $^{0.5}$/ft
$\dot{\eta}_1$	0	ft/s slugs $^{0.5}$/ft
η_2	0.7967	ft slugs $^{0.5}$/ft
$\dot{\eta}_2$	0	ft/s slugs $^{0.5}$/ft

$$
\begin{aligned}
\dot{L}_{\bar{Q}} \leq & -k_h z_h^2 - k_\gamma z_\gamma^2 - k_\theta z_\theta^2 - k_Q z_Q^2 - \frac{\Gamma_h \tilde{V}_m}{\mu_h}\tilde{\ell}_h^2 - \frac{\Gamma_\gamma g_{\gamma m}}{\mu_\gamma}\tilde{\ell}_\gamma^2 \\
& - \frac{\Gamma_\theta}{\mu_\theta}\tilde{\ell}_\theta^2 - \frac{\Gamma_Q \tilde{g}_{Qm}}{2\mu_Q}\tilde{\ell}_Q^2 - \frac{\omega_{\delta_e} c_Q}{2l_Q}\tilde{\vartheta}_Q^2 - \frac{b_Q}{2r_Q}\tilde{\xi}_Q^2 + \frac{\Gamma_h \tilde{V}_m}{\mu_h}\ell_h^2 \\
& + \frac{\Gamma_\gamma g_{\gamma m}}{\mu_\gamma}\ell_\gamma^2 + \frac{\Gamma_\theta}{\mu_\theta}\ell_\theta^2 + \frac{\Gamma_Q \tilde{g}_{Qm}}{2\mu_Q}\ell_Q^2 + \frac{\omega_{\delta_e} c_Q}{2l_Q}\vartheta_Q^2 + \frac{b_Q}{2r_Q}\xi_Q^2 \\
& + \frac{1}{2}\phi_h^2 + \frac{1}{2}\phi_\gamma^2 + \frac{1}{2}\phi_\theta^2 + \frac{1}{2}\phi_Q^2 + \tau_h + \tau_\gamma + \tau_\theta + \tau_Q + \underline{\omega}_{\delta_e}\sigma_Q \\
& + 0.2785 a_Q \xi_Q.
\end{aligned}
\tag{86}
$$

The whole FTFTC design for HFVs is shown in Figure 2.

4. Closed-Loop Stability Analysis

Theorem 14. *Despite the occurrence of unknown actuator fault (14), consider the closed-loop system composed by (15) and (16); the virtual control laws (64), (69), and (74); the intermediate control laws (44) and (81); the actual control laws (50) and (85); and the parameter adaptation laws (46)-(48), (65), (70), (75), and (82)–(84). Let Assumptions 1–4 hold. By designing the parameters properly, it therefore holds the following.*

The tracking errors e_V and e_h can converge into a predefined residual set within an user-defined time T.

(1) *The overshoot and convergence rate are guaranteed by FTPF, and all signals of the closed-loop system are SGPFS*

Proof. Take the Lyapunov function candidate as

$$
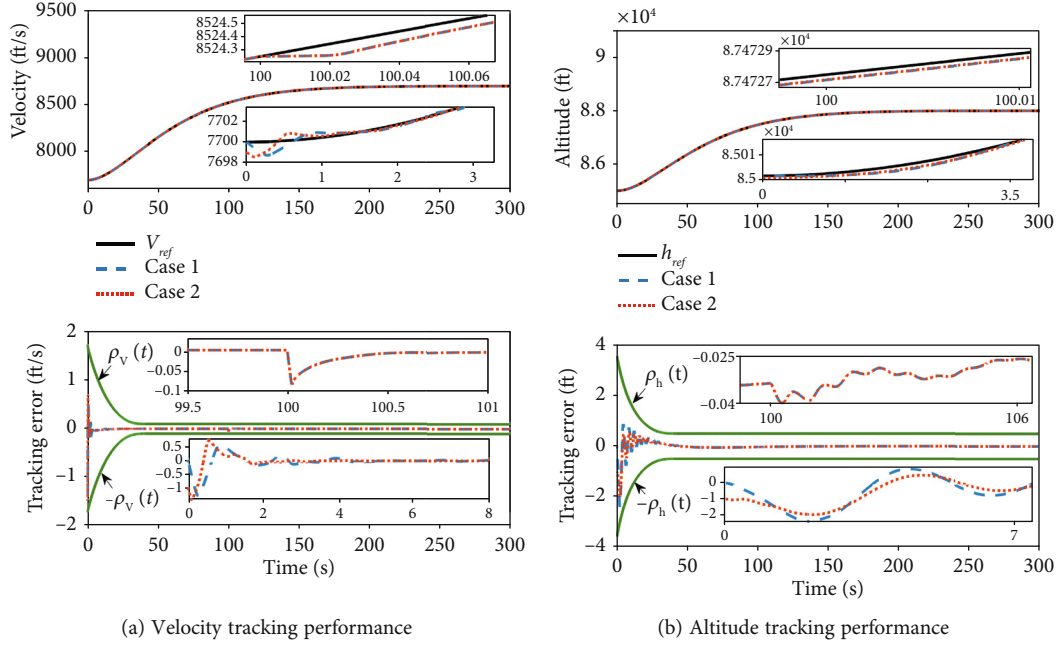L = L_{\bar{V}} + L_{\bar{Q}}.
\tag{87}
$$

Applying (54) and (86), the derivative of L gives

$$
\begin{aligned}
\dot{L} \leq & -k_V z_V^2 - k_h z_h^2 - k_\gamma z_\gamma^2 - k_\theta z_\theta^2 - k_Q z_Q^2 - \frac{\Gamma_V \tilde{g}_{Vm}}{2\mu_V}\tilde{\ell}_V^2 \\
& - \frac{\Gamma_h \tilde{V}_m}{\mu_h}\tilde{\ell}_h^2 - \frac{\Gamma_\gamma g_{\gamma m}}{\mu_\gamma}\tilde{\ell}_\gamma^2 - \frac{\Gamma_\theta}{\mu_\theta}\tilde{\ell}_\theta^2 - \frac{\Gamma_Q \tilde{g}_{Qm}}{2\mu_Q}\tilde{\ell}_Q^2 - \frac{\omega_\Phi c_V}{2l_V}\tilde{\vartheta}_V^2 \\
& - \frac{\omega_{\delta_e} c_Q}{2l_Q}\tilde{\vartheta}_Q^2 - \frac{b_V}{2r_V}\tilde{\xi}_V^2 - \frac{b_Q}{2r_Q}\tilde{\xi}_Q^2 + \frac{\Gamma_h \tilde{V}_m}{\mu_h}\ell_h^2 + \frac{\Gamma_\gamma g_{\gamma m}}{\mu_\gamma}\ell_\gamma^2 \\
& + \frac{\Gamma_\theta}{\mu_\theta}\ell_\theta^2 + \frac{\Gamma_V \tilde{g}_{Vm}}{2\mu_V}\ell_V^2 + \frac{\Gamma_Q \tilde{g}_{Qm}}{2\mu_Q}\ell_Q^2 + \frac{\omega_\Phi c_V}{2l_V}\vartheta_V^2 + \frac{\omega_{\delta_e} c_Q}{2l_Q}\vartheta_Q^2 \\
& + \frac{b_V}{2r_V}\xi_V^2 + \frac{b_Q}{2r_Q}\xi_Q^2 + \frac{1}{2}\phi_V^2 + \frac{1}{2}\phi_h^2 + \frac{1}{2}\phi_\gamma^2 + \frac{1}{2}\phi_\theta^2 + \frac{1}{2}\phi_Q^2 \\
& + \tau_V + \tau_h + \tau_\gamma + \tau_\theta + \tau_Q + \underline{\omega}_\Phi \sigma_V + \underline{\omega}_{\delta_e}\sigma_Q + 0.2785 a_V \xi_V \\
& + 0.2785 a_Q \xi_Q.
\end{aligned}
\tag{88}
$$

Recalling the definitions of $L_{\bar{V}}$ and $L_{\bar{Q}}$, the following inequation holds

$$
\dot{L} \leq -kL + C,
\tag{89}
$$

where $k = \min\{2k_V, 2k_h, 2k_\gamma, 2k_\theta, 2k_Q, \Gamma_V, \Gamma_h, \Gamma_\gamma, \Gamma_\theta, \Gamma_Q, b_V, b_Q, c_V, c_Q\}$, $C = (\Gamma_h \tilde{V}_m/\mu_h)\ell_h^2 + (\Gamma_\gamma g_{\gamma m}/\mu_\gamma)\ell_\gamma^2 + (\Gamma_\theta/\mu_\theta)\ell_\theta^2 + (\Gamma_V \tilde{g}_{Vm}/2\mu_V)\ell_V^2 + (\Gamma_Q \tilde{g}_{Qm}/2\mu_Q)\ell_Q^2 + (\underline{\omega}_\Phi c_V/2l_V)\vartheta_V^2 + (\underline{\omega}_{\delta_e} c_Q/2l_Q)\vartheta_Q^2 + (b_V/2r_V)\xi_V^2 + (b_Q/2r_Q)\xi_Q^2 + (1/2)\phi_V^2 + (1/2)\phi_h^2 + (1/2)\phi_\gamma^2 + (1/2)\phi_\theta^2 + (1/2)\phi_Q^2 + \tau_V + \tau_h + \tau_\gamma + \tau_\theta + \tau_Q + \underline{\omega}_\Phi \sigma_V + \underline{\omega}_{\delta_e}\sigma_Q + 0.2785 a_V \xi_V + 0.2785 a_Q \xi_Q$.

(a) Velocity tracking performance

(b) Altitude tracking performance

Figure 3: The velocity and altitude tracking performance under different initial states.
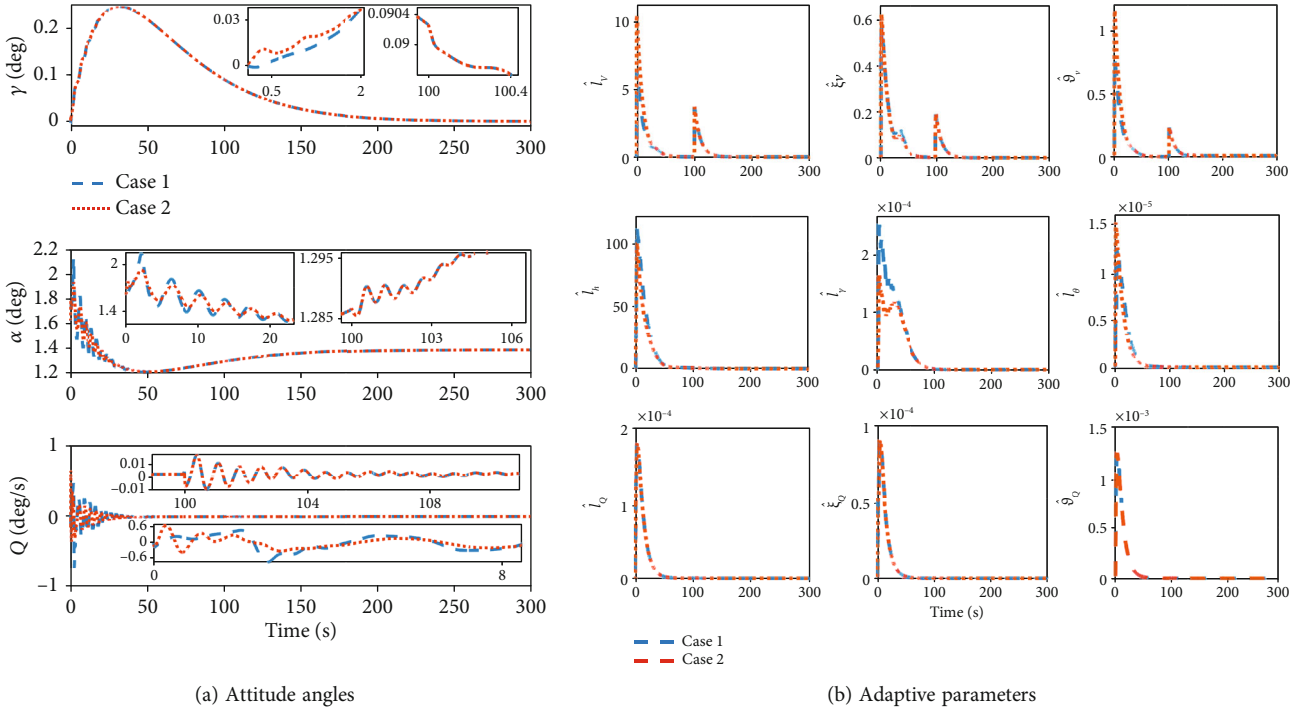
(a) Attitude angles

(b) Adaptive parameters

Figure 4: The attitude angles and adaptive parameters under different initial states.

Integrating both sides of (89) yields

$$L \leq L(0) + \frac{C}{k}. \tag{90}$$

In accordance with (34) and (60), we have

$$z_V \leq \sqrt{2L(0) + \frac{C}{k}}, z_h \leq \sqrt{2L(0) + \frac{C}{k}}, \tag{91}$$
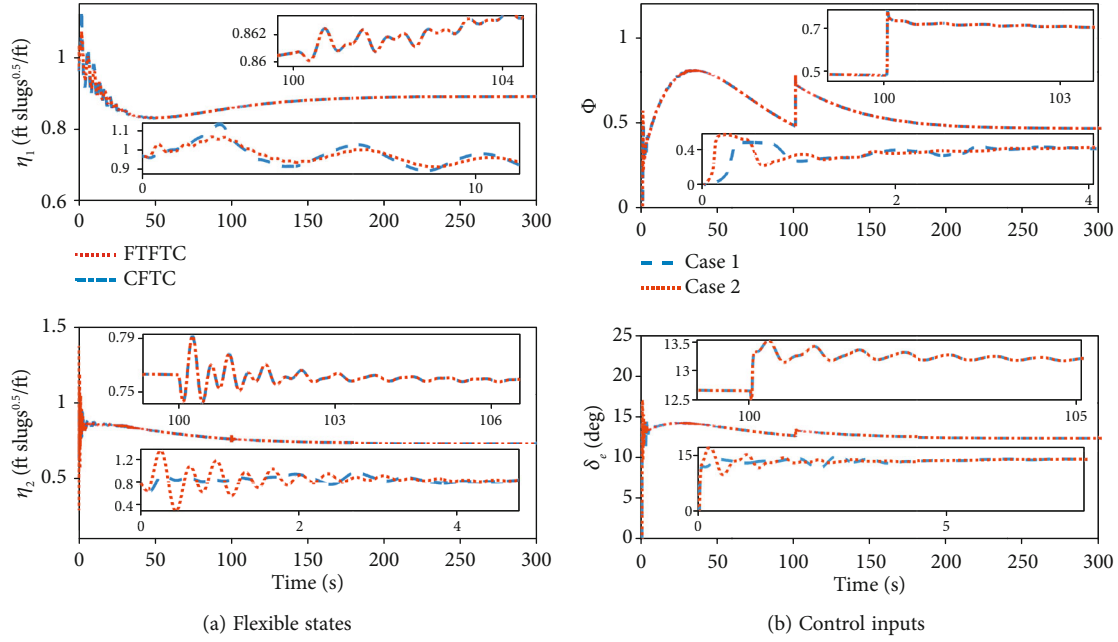
(a) Flexible states

(b) Control inputs

FIGURE 5: The flexible states and control inputs under different initial states.

In view of (42), (60), (67), (72), (77), (80), (87), and (90), the estimation errors of the adaptive parameters will converge to the following compact sets:

$$
\begin{cases}
\tilde{\ell}_V \leq \sqrt{2\mu_V\left(L(0) + \dfrac{C}{k}\right)} \\[2mm]
\tilde{\ell}_h \leq \sqrt{2\mu_h\left(L(0) + \dfrac{C}{k}\right)} \\[2mm]
\tilde{\ell}_\gamma \leq \sqrt{2\mu_\gamma\left(L(0) + \dfrac{C}{k}\right)} \\[2mm]
\tilde{\ell}_\theta \leq \sqrt{2\mu_\theta\left(L(0) + \dfrac{C}{k}\right)} \\[2mm]
\tilde{\ell}_Q \leq \sqrt{2\mu_Q\left(L(0) + \dfrac{C}{k}\right)}
\end{cases}
,\quad
\begin{cases}
\tilde{\vartheta}_V \leq \sqrt{\dfrac{2l_V}{\underline{\omega}_\Phi}\left(L(0) + \dfrac{C}{k}\right)} \\[3mm]
\tilde{\vartheta}_Q \leq \sqrt{\dfrac{2l_Q}{\underline{\omega}_{\delta_e}}\left(L(0) + \dfrac{C}{k}\right)} \\[3mm]
\tilde{\xi}_V \leq \sqrt{2r_V\left(L(0) + \dfrac{C}{k}\right)} \\[2mm]
\tilde{\xi}_Q \leq \sqrt{2r_Q\left(L(0) + \dfrac{C}{k}\right)}.
\end{cases}
\tag{92}
$$

Therefore, the transformational errors z_V and z_h are bounded. By reviewing (17)–(24), we can conclude that the velocity and altitude tracking errors converge to a residual set within a fixed time T and the prescribed performances are guaranteed. Besides, all signals of closed-loop system are SGPFS. According to the design of velocity controller (44), altitude controller (64), and the FTPF (17), the overshoots of velocity and altitude do not exceed their preset threshold. This completes the proof. + □

Remark 15. The existing fixed-time control strategies for HFVs [18–20] fail to take system transient and steady-state performances into account, and it is fairly complicated to make tracking error convergence into a preassigned compact set within the fixed time by selecting design parameters. It is worth noting that the fixed-time tracking control is achieved as long as the bounded condition is satisfied in the proposed design. Consequently, the complexity of the control structure is reduced and the initial states need not to be known accurately via the proposed control approach.

Remark 16. It is worth mentioning that the control performance is depended closely on the designed parameters of prescribed function. In (17), large initial errors are allowed by choosing a small enough r; larger ϑ and smaller T will increase the convergence rate. However, too large ϑ or too small T will give rise to actuator input saturations. In (44), (64), (69), (74), and (81), designed parameters k_V, τ_V, a_V, k_h, τ_h, k_γ, τ_γ, k_θ, τ_θ, k_Q, τ_Q, and a_Q determine the convergence rate and convergence accuracy. In (46)-(48), (65), (70), (75), and (82)–(84), designed parameters μ_V, Γ_V, r_V, b_V, l_V, c_V, μ_h, Γ_h, μ_γ, Γ_γ, μ_θ, Γ_θ, μ_Q, Γ_Q, r_Q, b_Q, l_Q, and c_Q effect convergence rate of the adaptive parameters. In the controller design, we need to design the parameters properly to improve the tracking performance and avoid the saturation phenomenon.

Remark 17. When the actuator failure occurs, the upper and lower bounds of fault parameters are estimated by

(a) Velocity tracking performance
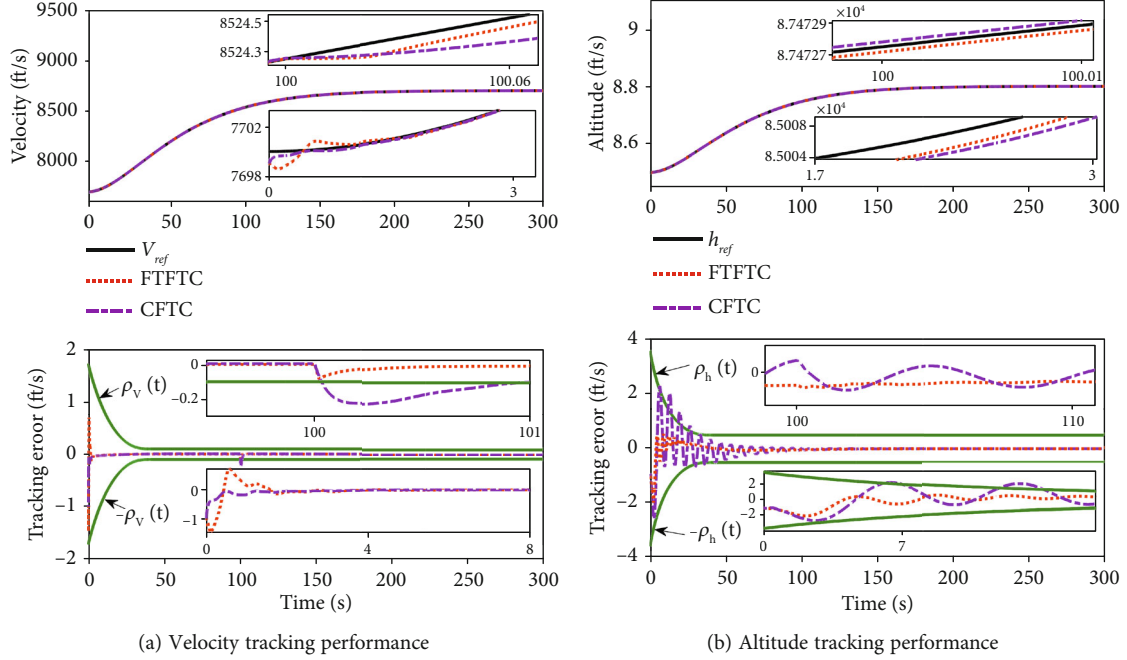
(b) Altitude tracking performance

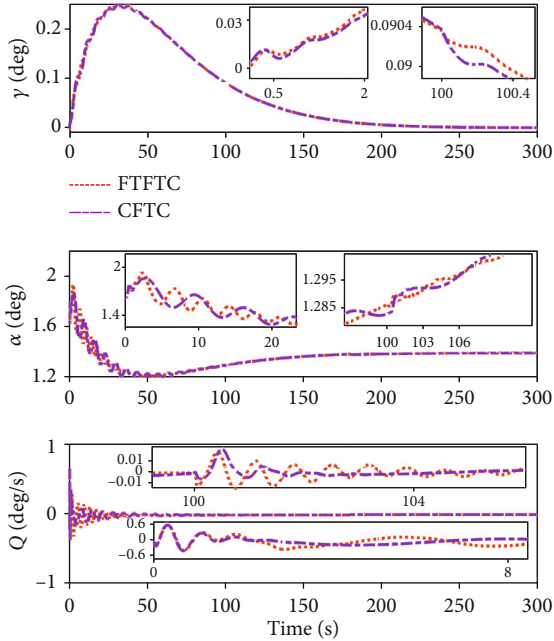Figure 6: The velocity and altitude tracking performance via different methodologies.

Figure 7: The attitude angles via different methodologies.

the adaptive laws (47), (48), (83), and (84), then the intermediate control laws (44) and (81) and the actual control laws (50) and (85) are executed. By this way, the flight control system is robust to actuator failure. Compared with the state-of-the-art FTC methods [30–33], the fixed-time stability is guaranteed, and the prescribed performance is ensured.

5. Simulations

In this section, simulation results are used to demonstrate the effectiveness and superiority of the proposed methodology. The model parameters of HFVs can be consulted from [40]. HFVs are expected to climb a maneuver from the initial trim conditions, depicted in Table 1, to the final values $V = 8700\text{ft/s}$ and $h = 88000\text{ft}$. The external disturbances in velocity subsystem and altitude subsystem are set as $d_V = \sin(0.1\pi t)\text{ft/s}$, $d_\gamma = 0.001\sin(0.01\pi t)$ deg, $d_Q = 0.01\sin(0.01\pi t)$ deg/s. The reference trajectories of velocity and altitude are generated via the following filters [11]:

$$
\begin{aligned}
\frac{V_{ref}(s)}{V_c(s)} &= \frac{0.03^2}{s^2 + 2 \times 0.95 \times 0.03 \times s + 0.03^2}, \\
\frac{h_{ref}(s)}{h_c(s)} &= \frac{0.03^2}{s^2 + 2 \times 0.95 \times 0.03 \times s + 0.03^2},
\end{aligned}
\tag{93}
$$

where $V_{ref}(s)$ and $h_{ref}(s)$ represent the inputs of filters and $V_c(s)$ and $h_c(s)$ represent the outputs of filters, respectively. It is assumed that HFVs actuators failed at 100 s and the details of failure are formulated in the form of

$$
\begin{aligned}
v(\Phi) &= 0.8\Phi - 0.1, \\
v(\delta_e) &= 0.8\delta_e + 0.0349.
\end{aligned}
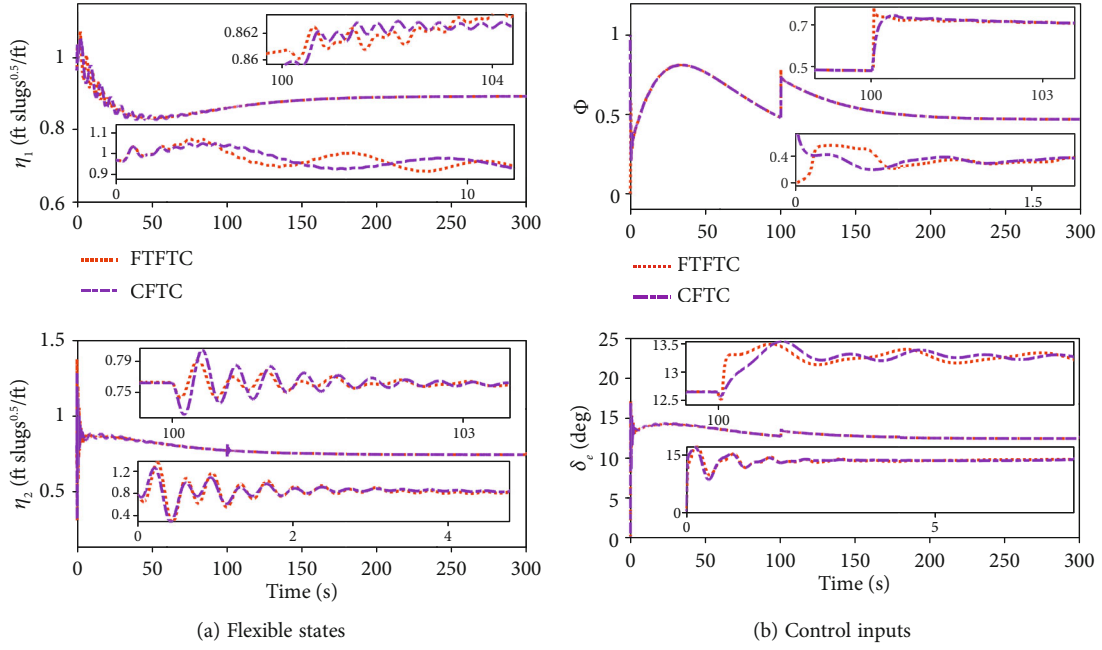\tag{94}
$$

(a) Flexible states
(b) Control inputs

FIGURE 8: The flexible states and control inputs via different methodologies.
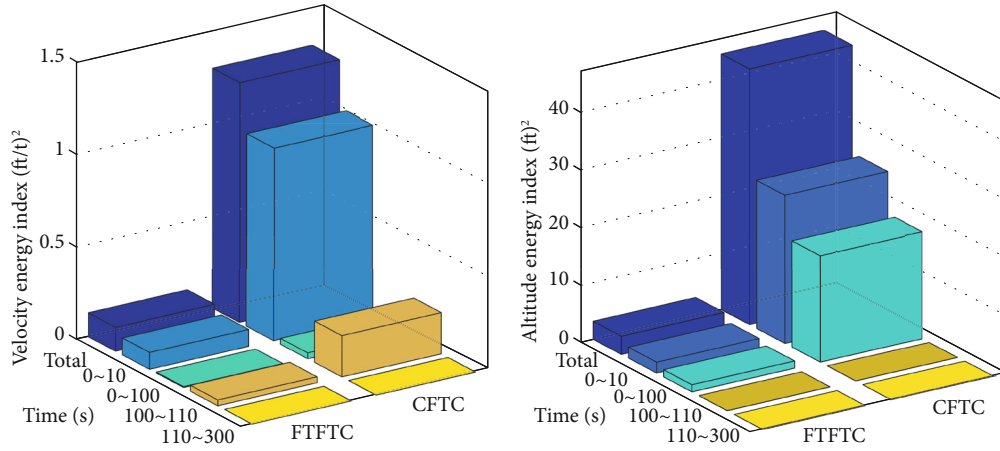

FIGURE 9: The performance indexes via different methodologies.

The FTPFs are selected as

$$\rho_V(t) = \begin{cases} \coth\left(\dfrac{t}{50-t} + 0.4\right) - 0.9, & 0 \le t < 50 \\ 0.1, & t \ge 50, \end{cases}$$

$$\rho_h(t) = \begin{cases} \coth\left(\dfrac{t}{50-t} + 0.4\right) - 0.5, & 0 \le t < 50 \\ 0.5, & t \ge 50. \end{cases}$$

(95)

The fuzzy rules in $\boldsymbol{W}_V^{*\mathrm{T}} \boldsymbol{S}_V$ are listed as

$\mathcal{R}^l$: If V is F_V^i, then y is B^l, where $i = 1, 2, 3$ and $l = 1, 2, 3$.

The fuzzy rules in $\boldsymbol{W}_\gamma^{*\mathrm{T}} \boldsymbol{S}_\gamma$ are listed as

TABLE 2: The performance index of control inputs.

Control method	Performance index of Φ	Performance index of δ_e
FTFTC	99.4683	15.2615
CFTC	99.4574	15.2620

$\mathcal{R}^l$: If h is F_h^i, and γ is F_γ^j, then y is B^l, where $i = 1, 2, 3$; $j = 1, 2, 3$; and $l = 1, 2, \cdots, 9$.

Then, the fuzzy rules in $\boldsymbol{W}_\theta^{*\mathrm{T}} \boldsymbol{S}_\theta$ are listed as

$\mathcal{R}^l$: If h is F_h^i, and γ is F_γ^j, and θ is F_θ^k, then y is B^l, where $i = 1, 2, 3$; $j = 1, 2, 3$; $k = 1, 2, 3$; and $l = 1, 2, \cdots, 27$.

The fuzzy rules in $\boldsymbol{W}_Q^{*\mathrm{T}} \boldsymbol{S}_Q$ are listed as

$\mathscr{R}^l$: If h is F_h^i, and γ is F_γ^j, and θ is F_θ^k, and Q is F_Q^p, then y is B^l, where $i = 1, 2, 3$; $j = 1, 2, 3$; $k = 1, 2, 3$; $p = 1, 2, 3$; and $l = 1, 2, \cdots, 81$.

The fuzzy membership function is given as follows:

$$
\begin{aligned}
1\mu_{F_V^1} &= \exp\left[-(V - 7500)^2/300\right], \\
\mu_{F_V^2} &= \exp\left[-(V - 8100)^2/300\right], \\
\mu_{F_V^3} &= \exp\left[-(V - 8700)^2/300\right], \\
\mu_{F_h^1} &= \exp\left[-(h - 85000)^2/1000\right], \\
\mu_{F_h^2} &= \exp\left[-(h - 87000)^2/1000\right], \\
\mu_{F_h^3} &= \exp\left[-(h - 89000)^2/1000\right], \\
\mu_{F_\gamma^1} &= \exp\left[-(\gamma - 0)^2/0.0005\right], \\
\mu_{F_\gamma^2} &= \exp\left[-(\gamma - 0.005)^2/0.0005\right], \qquad (96) \\
\mu_{F_\gamma^3} &= \exp\left[-(\gamma - 0.01)^2/0.0005\right], \\
1\mu_{F_\theta^1} &= \exp\left[-(\theta - 0)^2/0.002\right], \\
\mu_{F_\theta^2} &= \exp\left[-(\theta - 0.02)^2/0.002\right], \\
\mu_{F_\theta^3} &= \exp\left[-(\theta - 0.04)^2/0.002\right], \\
\mu_{F_Q^1} &= \exp\left[-(Q + 0.03)^2/0.002\right], \\
\mu_{F_Q^2} &= \exp\left[-(Q - 0)^2/0.002\right], \\
\mu_{F_Q^3} &= \exp\left[-(Q - 0.03)^2/0.002\right].
\end{aligned}
$$

The controller parameters are selected as $k_V = \mu_V = r_V = l_V = \mu_h = \mu_\gamma = \mu_\theta = \mu_Q = r_Q = l_Q = 1$, $\tilde{g}_{Vm} = 0.00001$, $\tilde{g}_{Qm} = 1$, $\tau_V = \Gamma_V = c_V = b_V = \tau_h = \Gamma_h = \tau_\gamma = \Gamma_\gamma = \tau_\theta = \Gamma_\theta = \tau_Q = \Gamma_Q = c_Q = b_Q = 0.1$, $a_V = 0.2$, $a_Q = 0.25$, $\sigma_V = \sigma_Q = (1/(t^2 + 0.01))$, $k_h = 10$, $k_\gamma = 2$, $k_\theta = 10$, and $k_Q = 50$. Taking the engineering practice into account, the limitations of the actuators are set as $\Phi \in [0, 1]$, $\delta_e \in [-20 \text{ deg}, 20 \text{ deg}]$ [40]. To prove that the proposed FTFTC is realizable and independent of the initial states, the first example is taken, while the superiority of the proposed FTFTC over the conventional fixed-time control (CFTC) in [49] is explained in the second example.

Example 18. In this example, two different initial states cases, i.e., case 1 ($e_V(0) = e_h(0) = 0$) and case 2 ($e_V(0) = e_h(0) = 1$), are considered, respectively.

The obtained simulation results, depicted in Figures 3–5, reveal that the proposed FTFTC has full capabilities to deal with the condition that aerodynamic parameters are perturbed and initial states are uncertain. It can be observed from Figures 3(a)–3(b) that the velocity and altitude tracking errors are guaranteed not to exceed the prescribed bounds. Furthermore, the velocity and altitude can rapidly track their reference trajectories even if the actuator fails.

Figures 4(a) and 5(a) depict that there is no high-frequency chattering in the attitude angles as well as the flexible states, and they can converge to their steady values rapidly. Figure 5(b) shows that the control inputs are smooth and within realistic limits. The estimated values of adaptive parameters are bounded, which is presented in Figure 4(b).

Example 19. In this example, simulations via the CFTC [49] and the proposed FTFTC are demonstrated, where the initial states are set as $e_V(0) = e_h(0) = 1$. In order to expound the advantages of tracking performances of the proposed FTFTC, the performance index of tracking error $E_e = \int_0^t e^2 \mathrm{d}t$ is introduced where e denotes the tracking error. In order to compare the energy consumption between the FTFTC and CFTC, the performance index of control input $E_u = \int_0^t u^2 \mathrm{d}t$ is defined where u denotes the control input.

Simulation results are depicted in Figures 6–9. Figures 6(a)–6(b) shows the velocity and altitude tracking performance, in which the velocity and altitude tracking errors are limited in the preset bounds by the proposed FTFTC and the proposed FTFTC can provide higher rate of convergence compared with the CFTC. Besides, the attitude angles and flexible states are shown in Figures 7 and 8(a), indicating that smaller oscillation amplitudes of attitude angles and flexible states are achieved in the presence of actuator failures by means of the proposed FTFTC. Figure 8(b) shows that the control inputs are smooth and within realistic limits by means of the proposed method. In addition, Figure 9 gives that less error energy is produced via the proposed FTFTC in contrast with the CFTC. Table 2 shows that the energy consumption of actuator with FTFTC is almost equal to that with CFTC. That is to say, the proposed FTFTC can achieve more accurate tracking.

6. Conclusions

A novel fixed-time fuzzy adaptive fault-tolerant control methodology based on performance function is developed for hypersonic flight vehicles in this work. In contrast with the conventional fixed-time control, the proposed approach not only guarantees that the velocity and altitude tracking errors converge into a preassigned compact set, but also satisfies both the prescribed transient and steady performance. In addition, the proposed scheme can avoid the singularity problem caused by the differential of fractional order tracking error and remain valid in spite of actuator faults. Comparative simulation results confirm the validity and superiority of the presented control strategy. Note that the distributed adaptive containment fault-tolerant control of multi-HFVs formation is an important research region for the future [50–53]; thus, the extension of our control scheme to the case of multi-HFVs formation will be an interesting topic for further investigation.

Abbreviations

V: Velocity
θ: Pitch angle

α: Angle of attack
T: Thrust
L: Lift
I_{yy}: Moment of inertia
Φ: Fuel equivalence ratio
z_T: Thrust moment arm
N_i^0: Constant term in N_i
C_L^0: Constant term in L
$C_L^{\delta_e}$: Coefficient of δ_e in L
h: Altitude
γ: Flight path angle
Q: Pitch rate
D: Drag
M: Pitching moment
m: Vehicle mass
δ_e: Elevator angular deflection
N_i: i-th generalized force
$N_i^{\delta_e}$: Contribution of δ_e to N_i
$C_{M,\alpha}^0$: Constant term in M
C_L^α: Coefficient of α in L
$\bar{c}$: Mean aerodynamic chord
η_i: i-th generalized flexible coordinate
S: Reference area
$\bar{q}$: Dynamic pressure
ζ_i: Damping ratio for flexible mode η_i
$C_D^{\delta_e^i}$: i-th order coefficient of δ_e in D
$C_D^{\alpha^i}$: i-th order coefficient of α in D
C_D^0: Constant term in D
$N_i^{\alpha^j}$: j-th order contribution of α to N_i
$C_{M,\alpha}^{\alpha^i}$: i-th order coefficient of α in M
ω_i: Natural frequency for η_i.

Data Availability

The data used to support the findings of this study are available from the corresponding author upon request.

Conflicts of Interest

The authors declare that there is no conflict of interest regarding the publication of this article.

Acknowledgments

References

[1] Z. Dong, Y. Li, M. Lv, and R. Zuo, "Adaptive accurate tracking control of HFVs in the presence of dead-zone and hysteresis input nonlinearities," *Chinese Journal of Aeronautics*, vol. 34, no. 5, pp. 642–651, 2021.

[2] L. Fiorentini and A. Serrani, "Adaptive restricted trajectory tracking for a non-minimum phase hypersonic vehicle model," *Automatica*, vol. 48, no. 7, pp. 1248–1261, 2012.

[3] Q. Shen, B. Jiang, and V. Cocquempot, "Fault tolerant control for T-S fuzzy systems with application to near space hypersonic vehicle with actuator faults," *IEEE Transactions on Fuzzy Systems*, vol. 20, no. 4, pp. 652–665, 2012.

[4] H. Wu, Z. Liu, and L. Guo, "Robust $ L_ {\bm\infty} $-Gain fuzzy disturbance observer-based control design with adaptive bounding for a hypersonic vehicle," *IEEE Transactions on Fuzzy Systems*, vol. 22, no. 6, pp. 1401–1412, 2014.

[5] X. Cheng, P. Wang, and G. Tang, "Fuzzy-reconstruction-based robust tracking control of an air-breathing hypersonic vehicle," *Aerospace Science and Technology*, vol. 86, pp. 694–703, 2019.

[6] Y. Cheng, B. Xu, F. Wu, X. Hu, and R. Hong, "HOSM observer based robust adaptive hypersonic flight control using composite learning," *Neurocomputing*, vol. 295, pp. 98–107, 2018.

[7] X. Hu, B. Xu, and C. Hu, "Robust adaptive fuzzy control for HFV with parameter uncertainty and unmodeled dynamics," *IEEE Transactions on Industrial Electronics*, vol. 65, no. 11, pp. 8851–8860, 2018.

[8] X. Bu, G. He, and K. Wang, "Tracking control of air-breathing hypersonic vehicles with non-affine dynamics via improved neural back-stepping design," *ISA Transactions*, vol. 75, pp. 88–100, 2018.

[9] B. Xu, D. Wang, F. Sun, and Z. Shi, "Direct neural discrete control of hypersonic flight vehicle," *Nonlinear Dynamics*, vol. 70, no. 1, pp. 269–278, 2012.

[10] J. Wang and H. Wu, "Exponentially stabilizing fuzzy controller design for a nonlinear ODE-beam cascaded system and its application to flexible air-breathing hypersonic vehicle," *Fuzzy Sets & Systems*, vol. 385, no. 15, pp. 127–147, 2020.

[11] X. Bu, X. Wu, F. Zhu, J. Huang, Z. Ma, and R. Zhang, "Novel prescribed performance neural control of a flexible air-breathing hypersonic vehicle with unknown initial errors," *ISA Transactions*, vol. 59, pp. 149–159, 2015.

[12] X. Bu, Y. Xiao, and K. Wang, "A prescribed performance control approach guaranteeing small overshoot for air-breathing hypersonic vehicles via neural approximation," *Aerospace Science and Technology*, vol. 71, pp. 485–498, 2017.

[13] Z. Yu, Y. Zhang, B. Jiang, J. Fu, Y. Jin, and T. Chai, "Composite adaptive disturbance observer-based decentralized fractional-order fault-tolerant control of networked UAVs," *IEEE Transactions on Systems, Man, and Cybernetics: Systems*, vol. 52, no. 2, pp. 799–813, 2022.

[14] H. Sun, S. Li, and C. Sun, "Finite time integral sliding mode control of hypersonic vehicles," *Nonlinear Dynamics*, vol. 73, no. 1-2, pp. 229–244, 2013.

[15] J. Sun, J. Yi, Z. Pu, and Z. Liu, "Adaptive fuzzy nonsmooth backstepping output-feedback control for hypersonic vehicles with finite-time convergence," *IEEE Transactions on Fuzzy Systems*, vol. 28, no. 10, pp. 2320–2334, 2020.

[16] C. Dong, Y. Liu, and Q. Wang, "Barrier Lyapunov function based adaptive finite-time control for hypersonic flight vehicles with state constraints," *ISA Transactions*, vol. 96, pp. 163–176, 2020.

[17] M. Basin, P. Yu, and Y. Shtessel, "Hypersonic missile adaptive sliding mode control using finite- and fixed-time observers," *IEEE Transactions on Industrial Electronics*, vol. 65, no. 1, pp. 930–941, 2018.

[18] M. Chen, H. Wang, and X. Liu, "Adaptive fuzzy practical fixed-time tracking control of nonlinear systems," *IEEE Transactions on Fuzzy Systems*, vol. 29, no. 3, pp. 664–673, 2021.

[19] X. Yu, P. Li, and Y. Zhang, "Fixed-time actuator fault accommodation applied to hypersonic gliding vehicles," *IEEE Transactions on Automation science and Engineering*, vol. 18, no. 3, pp. 1429–1440, 2021.

[20] J. Sun, J. Yi, and Z. Pu, "Augmented fixed-time observer-based continuous robust control for hypersonic vehicles with measurement noises," *IET Control Theory & Applications*, vol. 13, no. 3, pp. 422–433, 2019.

[21] B. Jiang, Q. Hu, and M. Friswell, "Fixed-time attitude control for rigid spacecraft with actuator saturation and faults," *IEEE Transactions on Control Systems Technology*, vol. 24, no. 5, pp. 1892–1898, 2016.

[22] Y. Li, K. Li, and S. Tong, "Finite-time adaptive fuzzy output feedback dynamic surface control for MIMO nonstrict feedback systems," *IEEE Transactions on Fuzzy Systems*, vol. 27, no. 1, pp. 96–110, 2019.

[23] Y. Li, X. Shao, and S. Tong, "Adaptive fuzzy prescribed performance control of nontriangular structure nonlinear systems," *IEEE Transactions on Fuzzy Systems*, vol. 28, no. 10, pp. 2416–2426, 2020.

[24] M. Lv, S. Baldi, and Z. Liu, "The non-smoothness problem in disturbance observer design: a set-invariance-based adaptive fuzzy control method," *IEEE Transactions on Fuzzy Systems*, vol. 27, no. 3, pp. 598–604, 2019.

[25] M. Lv, B. Schutter, W. Yu, W. Zhang, and S. Baldi, "Nonlinear systems with uncertain periodically disturbed control gain functions: adaptive fuzzy control with invariance properties," *IEEE Transactions on Fuzzy Systems*, vol. 28, no. 4, pp. 746–757, 2020.

[26] Y. Li, N. Xu, B. Niu, Y. Chang, J. Zhao, and X. Zhao, "Small-gain technique-based adaptive fuzzy command filtered control for uncertain nonlinear systems with unmodeled dynamics and disturbances," *International Journal of Adaptive Control and Signal Processing*, vol. 35, no. 9, pp. 1664–1684, 2021.

[27] F. Tang, B. Niu, H. Wang, L. Zhang, and X. Zhao, "Adaptive fuzzy tracking control of switched MIMO nonlinear systems with full state constraints and unknown control directions," *IEEE Transactions on Circuits and Systems-II: Express Briefs*, vol. 69, no. 6, pp. 2912–2916, 2022.

[28] H. Liang, Z. Du, T. Huang, and Y. Pan, "Neuroadaptive performance guaranteed control for multiagent systems with power integrators and unknown measurement sensitivity," in *IEEE Transactions on Neural Networks and Learning Systems*, 2022.

[29] H. Liang, G. Liu, H. Zhang, and T. Huang, "Neural-network-based event-triggered adaptive control of nonaffine nonlinear multiagent systems with dynamic uncertainties," *IEEE Transactions on Neural Networks and Learning Systems*, vol. 32, no. 5, pp. 2239–2250, 2021.

[30] O. Mofid and S. Mobayen, "Adaptive finite-time backstepping global sliding mode tracker of quad-rotor UAVs under model uncertainty, wind perturbation, and input saturation," *IEEE Transactions on Aerospace and Electronic Systems*, vol. 58, no. 1, pp. 140–151, 2022.

[31] O. Mofid, S. Mobayen, and W. Wong, "Adaptive terminal sliding mode control for attitude and position tracking control of quadrotor UAVs in the existence of external disturbance," *IEEE Access*, vol. 9, pp. 3428–3440, 2021.

[32] O. Mofid, S. Mobayen, C. Zhang, and B. Esakki, "Desired tracking of delayed quadrotor UAV under model uncertainty and wind disturbance using adaptive super-twisting terminal sliding mode control," *ISA Transactions*, vol. 123, pp. 455–471, 2022.

[33] Z. Yu, Y. Zhang, B. Jiang et al., "Enhanced recurrent fuzzy neural fault-tolerant synchronization tracking control of multiple unmanned airships via fractional calculus and fixed-time prescribed performance function," in *IEEE Transactions on Fuzzy Systems*, 2022.

[34] Z. Yu, Y. Zhang, B. Jiang et al., "Fractional-order adaptive fault-tolerant synchronization tracking control of networked fixed-wing UAVs against actuator-sensor faults via intelligent learning mechanism," *IEEE Transactions on Neural Networks and Learning Systems*, vol. 32, no. 12, pp. 5539–5553, 2021.

[35] Y. Li, "Finite time command filtered adaptive fault tolerant control for a class of uncertain nonlinear systems," *Automatica*, vol. 106, no. 4, pp. 117–123, 2019.

[36] Y. Li and G. Yang, "Adaptive asymptotic tracking control of uncertain nonlinear systems with input quantization and actuator faults," *Automatica*, vol. 72, pp. 177–185, 2016.

[37] H. Sun, S. Li, and C. Sun, "Adaptive fault-tolerant controller design for airbreathing hypersonic vehicle with input saturation," *Journal of Systems Engineering and Electronics*, vol. 24, no. 3, pp. 488–499, 2013.

[38] C. Benchlioulis and G. Rovithakis, "Adaptive control with guaranteed transient and steady state tracking error bounds for strict feedback systems," *Automatica*, vol. 45, no. 2, pp. 532–538, 2009.

[39] Z. Dong, Y. Li, M. Lv, J. Park, and D. Sun, *Fixed-time fuzzy adaptive fault-tolerant control for hypersonic flight vehicles using a new prescribed performance function*, Research Square, 2021.

[40] J. Parker, A. Serrani, S. Yurkovich, M. Bolender, and D. Doman, "Control-oriented modeling of an air-breathing hypersonic vehicle," *Journal of Guidance Control and Dynamics*, vol. 30, no. 3, pp. 856–869, 2007.

[41] L. Fiorentini, A. Serrani, M. Bolender, and D. Doman, "Nonlinear robust adaptive control of flexible air-breathing hypersonic vehicles," *Journal of Guidance Control & Dynamics*, vol. 32, no. 2, pp. 402–417, 2009.

[42] B. Xu, D. Wang, Y. Zhang, and Z. Shi, "DOB-based neural control of flexible hypersonic flight vehicle considering wind effects," *IEEE Transactions on Industrial Electronics*, vol. 64, no. 11, pp. 8676–8685, 2017.

[43] B. Xu, Z. Shi, F. Sun, and W. He, "Barrier lyapunov function based learning control of hypersonic flight vehicle with AOA constraint and actuator faults," *IEEE Transactions on Cybernetics*, vol. 49, no. 3, pp. 1047–1057, 2019.

[44] L. Yang, X. Liu, and Y. Jing, "Adaptive neural networks finite-time tracking control for non-strict feedback systems via prescribed performance," *Information Sciences*, vol. 468, pp. 29–46, 2018.

[45] Y. Pan, Q. Li, H. Liang, and H. Lam, "A novel mixed control approach for fuzzy systems via membership functions online learning policy," *IEEE Transactions on Fuzzy Systems*, vol. 30, no. 9, pp. 3812–3822, 2022.

[46] Y. Pan, Y. Wu, and H. Lam, "Security-based fuzzy control for nonlinear networked control systems with DoS attacks via a resilient event-triggered scheme," in *IEEE Transactions on Fuzzy Systems*, 2022.

[47] Z. Liu, X. Dong, W. Xie, Y. Chen, and H. Li, "Adaptive fuzzy control for pure-feedback nonlinear systems with non-affine functions being semi-bounded and in-differentiable," *IEEE*

Transactions on Fuzzy Systems, vol. 26, no. 2, pp. 395–408, 2018.

[48] C. Wang and Z. Zuo, "Adaptive trajectory tracking control of output constrained multi-rotors systems," *IET Control Theory and Applications*, vol. 8, no. 13, pp. 1163–1174, 2014.

[49] X. Wang, J. Guo, S. Tang, and S. Qi, "Fixed-time disturbance observer based fixed-time back-stepping control for an air-breathing hypersonic vehicle," *ISA Transactions*, vol. 88, pp. 233–245, 2019.

[50] M. Lv, B. De Schutter, C. Shi, and S. Baldi, "Logic-based distributed switching control for agents in power chained form with multiple unknown control directions," *Automatica*, vol. 137, article 110143, 2022.

[51] M. Lv, W. Yu, J. Cao, and S. Baldi, "A separation-based methodology to consensus tracking of switched high-order nonlinear multi-agent systems," in *IEEE Transactions on Neural Networks and Learning Systems*, 2021.

[52] M. Lv, W. Yu, J. Cao, and S. Baldi, "Consensus in high-power multi-agent systems with mixed unknown control directions via hybrid nussbaum-based control. *IEEE transactions on*," *Cybernetics*, vol. 52, no. 6, pp. 5184–5196, 2022.

[53] M. Lv, B. De Schutter, and S. Baldi, "Non-recursive control for formation-containment of HFV swarms with dynamic event-triggered communication," in *IEEE Transactions on Industrial Informatics*, 2022.